Dalton Transactions

ROYAL SOCIETY OF CHEMISTRY

PAPER

View Article Online
View Journal | View Issue

Cite this: *Dalton Trans.*, 2023, **52**, 12098

Synthesis and cytotoxicity studies of Cu(I) and Ag(I) complexes based on sterically hindered β-diketonates with different degrees of fluorination†

Maura Pellei, *[a] Jo' Del Gobbo,[a] Miriam Caviglia,[a] Deepika V. Karade,[b] Valentina Gandin,[c] Cristina Marzano,*[c] Anurag Noonikara Poyil,[b] H. V. Rasika Dias *[b] and Carlo Santini [a]

Received 11th July 2023,
Accepted 1st August 2023

DOI: 10.1039/d3dt02179c

rsc.li/dalton

Design, synthesis, and *in vitro* antitumor properties of Cu(I) and Ag(I) phosphane complexes supported by the anions of sterically hindered β-diketone ligands, 1,3-dimesitylpropane-1,3-dione (HL^{Mes}) and 1,3-bis (3,5-bis(trifluoromethyl)phenyl)-3-hydroxyprop-2-en-1-one (HL^{CF3}) featuring trifluoromethyl or methyl groups on the phenyl moieties have been reported. In order to compare the biological effects of substituents on the phenyl moieties, the analogous copper(I) and silver(I) complexes of the anion of the parent 1,3-diphenylpropane-1,3-dione (HL^{Ph}) ligand were also synthesized and included in the study. In the syntheses of the Cu(I) and Ag(I) complexes, the phosphane coligands triphenylphosphine (PPh_3) and 1,3,5-triaza-7-phosphaadamantane (PTA) were used to stabilize silver and copper in the +1 oxidation state, preventing the metal ion reduction to Ag(0) or oxidation to Cu(II), respectively. X-ray crystal structures of HL^{CF3} and the metal adducts $[Cu(L^{CF3})(PPh_3)_2]$ and $[Ag(L^{Ph})(PPh_3)_2]$ are also presented. The antitumor properties of both classes of metal complexes were evaluated against a series of human tumor cell lines derived from different solid tumors, by means of both 2D and 3D cell viability studies. They display noteworthy antitumor properties and are more potent than cisplatin in inhibiting cancer cell growth.

Introduction

Medicinal inorganic chemistry allows the design of compounds with therapeutic properties that are not readily available in organic compounds.[1,2] Recently, many chelating ligands and delivery systems for metal-based drugs have been developed to obtain more potent, clinically effective, and less toxic metal-based antiproliferative drugs with improved selectivity towards tumour cells.[3,4] Group 11 metal complexes showed encouraging perspectives in this regard and several noble metal complexes were investigated for their antitumoral properties.[5–7]

β-Diketone compounds represent a very important class of reagents in the synthesis of heterocyclic compounds.[8] The β-diketone scaffold is not very common in nature though it is the main feature of curcumin and its derivatives.[9] Although β-diketones represent one of the oldest classes of chelating ligands,[10,11] their coordination chemistry continues to attract much interest, due to the ability of related metal complexes to support several unique and important catalytic reactions.[12] It is often noted that even modestly sterically hindered β-diketones offer improvements over the parent acetylacetone.[13] Truly hindered β-diketones have only recently been made synthetically accessible.[14] The presence of steric bulk on β-diketones is of great interest due to their peculiar coordination behavior useful for improving their catalytic activity and selectivity.[15,16] β-Diketonates have been used as supporting ligands for Ti(IV),[17,18] Ru(II),[19–25] Rh(I),[26,27] Pd(II)[28] and Pt-based anticancer agents.[29–33] They have also been reported to induce apoptosis in human tumor cells.[34] In an early investigation, several platinum(II) complexes with β-diketonate ligands as leaving groups were studied, revealing that the ligands play an integral role in modulating toxic side effects.[35] In particular, the phenyl ring substituents increase the lipophilicity and improve cellular uptake of the resulting com-

[a]*School of Science and Technology, Chemistry Division, University of Camerino, Via Madonna delle Carceri (ChIP), 62032 Camerino, Macerata, Italy. E-mail: maura.pellei@unicam.it*
[b]*Department of Chemistry and Biochemistry, The University of Texas at Arlington, Box 19065, Arlington, Texas 76019-0065, USA. E-mail: dias@uta.edu*
[c]*Department of Pharmaceutical and Pharmacological Sciences, University of Padova, via Marzolo 5, 35131 Padova, Italy. E-mail: cristina.marzano@unipd.it*

† Electronic supplementary information (ESI) available. CCDC 2279297–2279299. For ESI and crystallographic data in CIF or other electronic format see DOI: https://doi.org/10.1039/d3dt02179c

plexes, whereas the electron-withdrawing CF_3 group increases the hydrolysis rates of the complexes in aqueous solution.

Despite the enormous amount of work devoted to the synthesis and characterization of copper(II) β-diketonate complexes,[36] there are relatively few reports devoted to the corresponding Cu(I) complexes perhaps due to their tendency to undergo disproportionation to copper metal and copper(II) compounds in the absence of stabilizing ligands.[37,38] Reports of triorganophosphane adducts, (β-diketonate)$Cu(PR_3)_n$, are also relatively scarce.[39–52]

Several silver(I) β-diketonates have been synthesized and structurally characterized.[53–57] In particular, fluorinated β-diketonate ligands were used to construct coordination polymers,[58–60] stabilize multinuclear ethynide or thiolate clusters,[61,62] and as precursors for chemical vapor deposition processes.[63] Moreover, the photosensitivity of silver β-diketonates makes it possible to obtain functional materials even at room temperature.[64,65] However, very little attention has been paid to the study of phosphane adducts of silver(I) β-diketonates,[40,66–71] although they may also display a rich structural diversity.

To our knowledge, with the exception of Cu(II) derivatives of curcumin,[72,73] Casiopeinas®-like compounds (Cas III)[74–77] and analogous mixed 1,10-phenanthroline and 4,4,4-trifluoro-1-phenyl-1,3-butanedionate,[78] 2,2-bipyridine and 4,4,4-trifluoro-1-(2-furyl)-1,3-butanedionate[79,80] or benzoylacetonate,[81] acetylacetonate[82] and 2-thenoyltrifluoroacetonate,[83] very few studies on the anticancer activity of group 11 metal complexes of β-diketones have been reported in the literature to date.[84] Copper(I)- and silver(I)-based anticancer complexes supported by β-diketonate ligands remain an unexplored research field. Therefore, as part of our continuous investigation on the chemical and biological properties of copper- and silver-containing coordination compounds,[85–91] we report here for the first time a study on the syntheses, characterization and biological evaluation of new Ag(I) and Cu(I) complexes containing phosphanes and the anion of the β-diketone ligands, 1,3-dimesitylpropane-1,3-dione (HL^{Mes}), 1,3-bis(3,5-bis(trifluoromethyl)phenyl)-3-hydroxyprop-2-en-1-one (HL^{CF3}) and 1,3-diphenylpropane-1,3-dione (HL^{Ph}). The ligands were selected to systematically modify the electronic properties and hydrophobicity of the resulting metal complexes using phenyl, mesityl and trifluoromethyl-phenyl groups, respectively. On the other hand, fluorine-containing compounds are of relevant interest in modern medicinal chemistry and in general, they are of special interest for use in drug design because of the good biological activity and low toxicity of molecules containing the trifluoromethyl moieties.[92–94] Selective introduction of fluorine into a therapeutic or diagnostic small molecule candidate can enhance/modulate a number of physicochemical and pharmacokinetic properties such as improved metabolic stability and enhanced membrane permeation.[95] Indeed, the substitution of a main group by a trifluoromethyl group in a molecule might be expected to induce great changes in molecular properties, in terms of hydrophobicity, solubility and electronegativity affecting not only metabolic stability but also binding affinities toward target proteins.[96–99] In designing the novel β-diketonate metal complexes, the lipophilic triphenylphosphine (PPh_3) and hydrophilic 1,3,5-triaza-7-phosphaadamantane (PTA) were selected as co-ligands, in order to stabilize copper and silver in their +1 oxidation state and to confer different solubility properties to the corresponding metal complexes.

A search in the Cambridge Structural Database[100] reveals that many of the structurally well-authenticated phosphane adducts of copper(I) and silver(I) involve fluoroalkyl substituted β-diketonates. Among these, copper adducts are relatively more common and often feature two-phosphane ligands bonded to copper producing tetrahedral molecules. A relatively larger number of reported silver complexes are three-coordinate with one phosphane on silver(I). Two representative examples are depicted as **A** [52] and **B** [71] in Fig. 1.

Notably, structural data on copper and silver phosphane complexes supported by diaryl β-diketonates are quite limited. They include (1,3-diferrocenylpropane-1,3-dionato)bis(triphenylphosphine)copper(I) (**C**, Fig. 1),[50] (1,3-diphenyl-1,3-dionato)bis(triphenylphosphine)copper(I) (**D**, Fig. 1)[51] and (1,3-diphenyl-1,3-dionato)(trimethylphosphine)copper(I) (**E**, Fig. 1).[41] In this paper, we report the X-ray crystal structures of $[Cu(L^{CF3})(PPh_3)_2]$ and $[Ag(L^{Ph})(PPh_3)_2]$ as two new additions to this group.

Finally, the *in vitro* antitumor properties of the new Cu(I) and Ag(I) complexes as well as of the corresponding uncoordinated ligands were evaluated against several human cancer cell lines derived from different solid tumors by means of both 2D and 3D cell viability tests. The cytotoxicity data have been compared with those obtained with cisplatin, the reference metal-based chemotherapeutic drug.

Results and discussion

Synthesis and characterization

The β-diketones 1,3-bis(3,5-bis(trifluoromethyl)phenyl)propane-1,3-dione (HL^{CF3})[101] and 1,3-dimesityl-propane-1,3-dione (HL^{Mes})[102] were prepared according to the literature procedures and fully characterized by several methods. The X-ray crystal structure of HL^{CF3} is presented in the ESI (Fig. S1†). 1,3-Diphenylpropane-1,3-dione (HL^{Ph}) was obtained from commercial sources and used as received. β-Diketones are capable of keto–enol tautomerism, and the tautomers exist in equilibrium with each other in solution; although, in most organic solvents, β-diketones are predominately enolized.[103]

The sodium salts of β-diketonate ligand NaL^{CF3} (**1**), NaL^{Mes} (**2**) and NaL^{Ph} (**3**) were prepared, using a modified literature method of analogous sodium β-diketonates,[104] from the reaction with HL^{CF3}, HL^{Mes} and HL^{Ph} respectively, with NaOH in ethanol solution, and isolated as orange whitish solids in 85% yield for NaL^{CF3}, 74% yield for NaL^{Mes} and in 80% yield for NaL^{Ph} (Scheme 1).

Compounds **1**, **2** and **3** were fully characterized by multinuclear NMR spectroscopy, FT-IR, ESI-MS and elemental analysis. The two $(CF_3)_2Ph$, mesityl and phenyl groups are

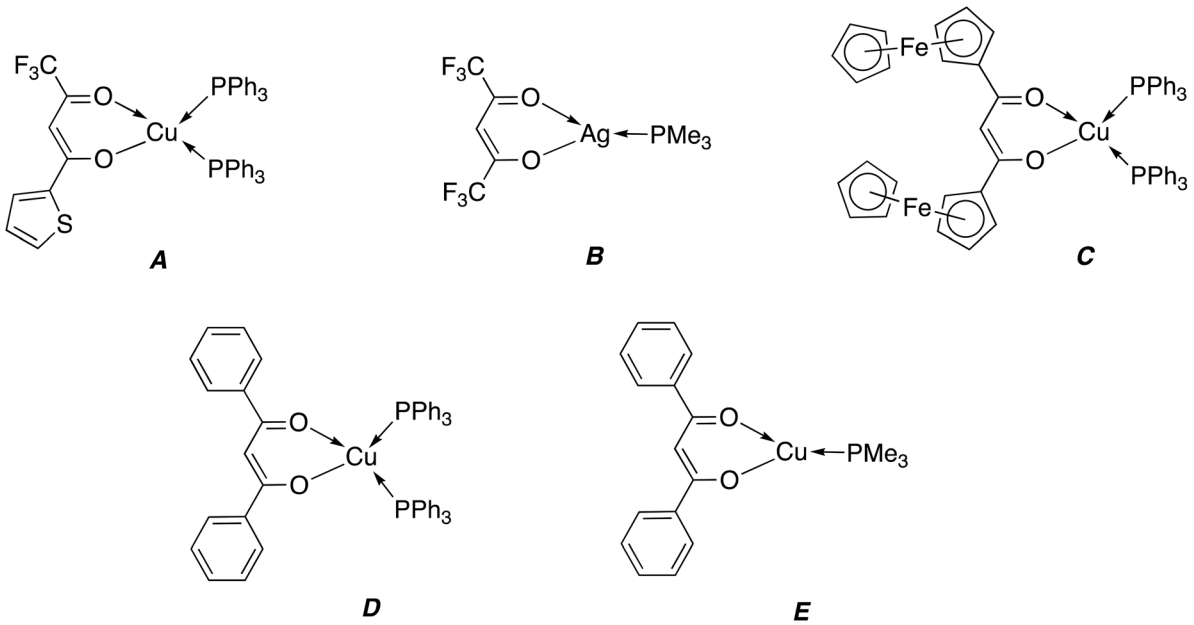

Fig. 1 Several examples of structurally authenticated copper(I) (A, C, D, E) and silver(I) (B) phosphane complexes.

magnetically equivalent in ^{1}H and ^{13}C NMR. The ^{1}H-NMR spectrum of **1**, recorded in DMSO-d_6 solution, shows a single set of resonances for the two C*H* protons in *ortho*- and *para*-positions of aromatic rings at 8.48 and 8.08 ppm, respectively, while the signal at δ 6.57 ppm is assignable to the COC*H*CO proton of the diketone. The ^{19}F NMR spectrum of **1** displayed a singlet at δ −61.21 ppm. Analogously, the ^{1}H NMR spectrum of compound **2** in $CDCl_3$ includes single peaks assignable to $(CH_3)_3$Ph protons (δ 2.23, 2.24 and 6.72 ppm) and to the COC*H*CO proton of the diketone (δ 5.31 ppm), while in the spectrum of **3** recorded in acetone-d_6 the aromatic protons are at 7.46–8.07 ppm and the COC*H*CO proton of the diketone is at δ 6.87 ppm. Deprotonation of β-diketonate ligands leads to a slight shift of the COC*H*CO group resonance with respect the protonated species (δ 6.89 ppm for HL^{CF3}, 5.77 ppm for HL^{Mes} and 6.89 for HL^{Ph}, in $CDCl_3$). The infrared (FT-IR) spectra of β-diketones generally exhibit very strong bands in the 1200–1650 cm^{-1} region.[105–108] For compounds **1–3**, the bands in the range of 1565–1643 cm^{-1} are assigned to the ν(C═O) stretching modes. For compound **1** the bands at 1163–1164 and 1110–1121 cm^{-1} can be assigned to the C–F stretching and CF_3 deformation, respectively.

For derivatives of the HL^{CF3} ligand, the Cu(I) complex [Cu$(L^{CF3})(PPh_3)_2$] (**4**) was prepared from the reaction of PPh_3, Cu$(CH_3CN)_4PF_6$ and the sodium salt NaL^{CF3}, while the Ag(I) complex [Ag$(L^{CF3})(PPh_3)_2$] (**5**) was prepared from the reaction of PPh_3, $AgNO_3$ and the sodium salt NaL^{CF3} (Scheme 1). The IR spectra recorded for a solid sample of **4** and **5** show all the expected bands for the β-diketone ligand and the triphenylphosphine co-ligands. The absorptions due to the C═O stretching are at 1582–1626 cm^{-1}, while bands due to C–F stretching and CF_3 deformation are at 1169–1171 and 1125–1126 cm^{-1}, respectively. They don't significantly vary with respect to the same absorptions of the carbonyl group detectable in the spectrum of the free ligand salt **1**. The ^{1}H-NMR spectra of complexes **4** and **5**, recorded in $CDCl_3$ solution at room temperature, show a single set of resonances for the β-diketone moiety, indicating that the protons of the aromatic rings are equivalent, with a slight shift due to the coordination to the metal centre. The PPh_3 co-ligands show a characteristic series of peaks in the range of 7.22–7.44 ppm. ^{19}F NMR spectra of **4** and **5** in $CDCl_3$ displayed singlets at δ −62.64 and −62.66 ppm, respectively. The ESI-MS study was performed by dissolving **4** and **5** in CH_3CN and recording the spectra in positive- and negative-ion modes. The structure of **4** and **5** was confirmed by the presence of peaks attributable to the [Cu(PPh_3) + $CH_3CN]^+$, [Cu$(PPh_3)_2]^+$, [Ag(PPh_3) + $CH_3CN]^+$ and [Ag$(PPh_3)_2]^+$ species, being positive fragments of the dissociation of the ligand from the complex. In addition, in the negative-ion mode spectra we observe peaks at 495 due to the $[L^{CF3}]^-$ fragment.

The Cu(I) complexes of HL^{Mes} and HL^{Ph} ligands, [Cu$(L^{Mes})(PPh_3)_2$] (**6**) and [Cu$(L^{Ph})(PPh_3)_2$] (**9**) were prepared from the reaction of PPh_3, Cu$(CH_3CN)_4PF_6$ and NaL^{Mes} (**2**) and NaL^{Ph} (**3**), respectively (Scheme 1). Analogously, the Ag(I) complexes [Ag$(L^{Mes})(PPh_3)_2$] (**7**) and [Ag$(L^{Ph})(PPh_3)_2$] (**10**) were prepared from the reaction of PPh_3, $AgNO_3$ and the sodium salts **2** and **3**, respectively (Scheme 1). The IR spectra recorded of solid samples of **6**, **7**, **9** and **10** show all the expected bands for the β-diketone ligand and the triphenylphosphine co-ligands. The absorptions due to the C═O stretching are at 1548–1651 cm^{-1} and they don't significantly vary with respect to the same absorptions in the spectra of the free ligand salts **2** and **3**. The ^{1}H-NMR spectra of complexes **6**, **7**, **9** and **10**, recorded in

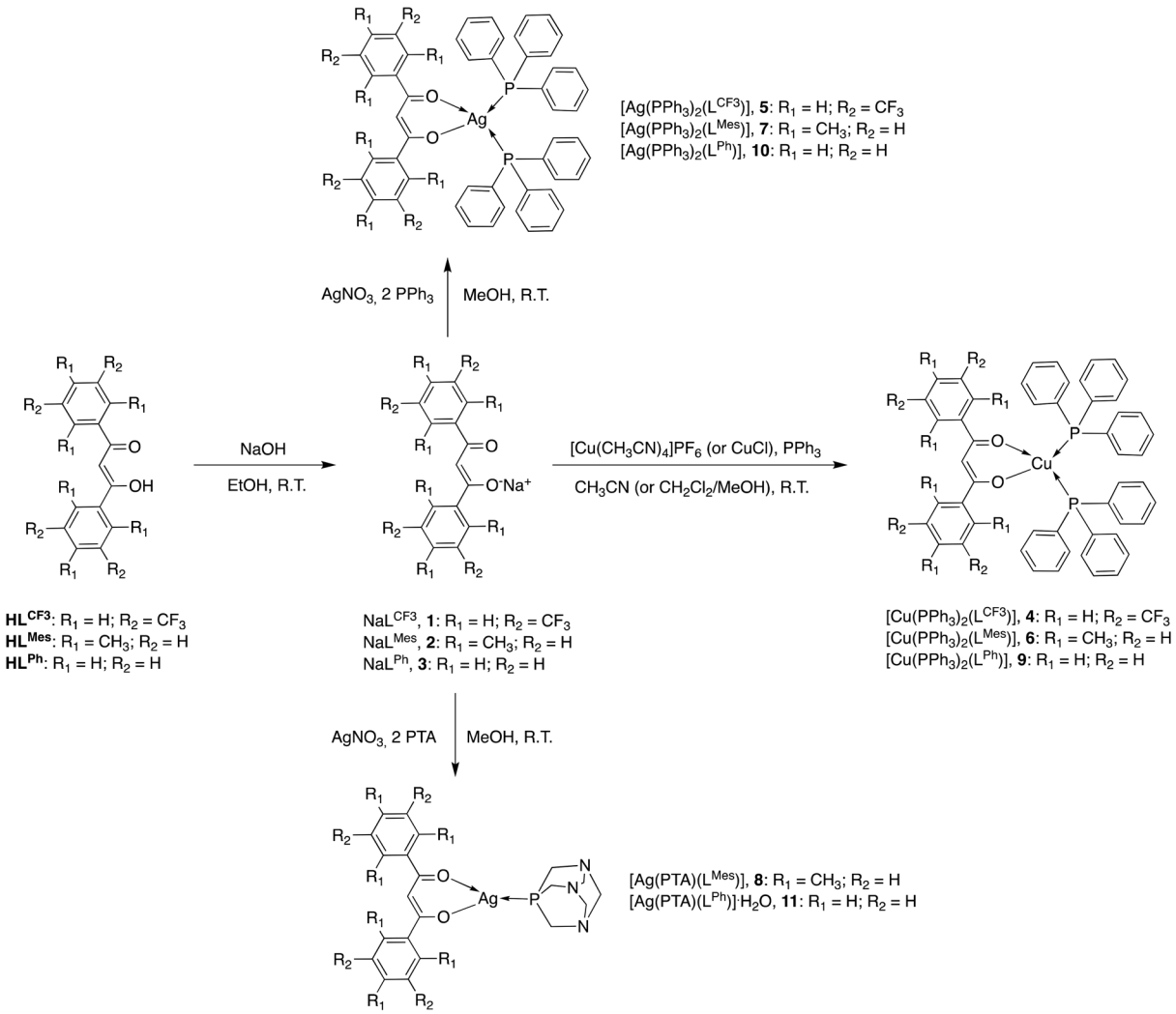

Scheme 1 Synthesis of compounds **1–11**.

$CDCl_3$ or CD_3OD solution at room temperature, show a single set of resonances for the β-diketone moiety, indicating that the protons of the aromatic rings are equivalent, with a slight shift due to coordination with the metal center. The PPh_3 co-ligands show a characteristic series of peaks in the range of 7.21–7.50 ppm. The ESI-MS study was performed by dissolving **6**, **7**, **9** and **10** in CH_2Cl_2/CH_3CN, CH_3OH or CH_3CN. In the positive-ion mode spectra, we observed the presence of peaks attributable to the $[Cu(PPh_3)_2]^+$ and $[Ag(PPh_3)_2]^+$ species, which are positive fragments of the dissociation of the ligand from the complexes. In addition, in the negative-ion mode spectra we observed peaks at *m*/*z* 307 and 223, due to the $[L^{Mes}]^-$ and $[L^{Ph}]^-$ fragments, respectively.

The Ag(I) complexes of HL^{Mes} and HL^{Ph} ligands, $[Ag(L^{Mes})(PTA)]$ (**8**) and $[Ag(L^{Ph})(PTA)]\cdot H_2O$ (**11**), were prepared from the reaction of PTA, $AgNO_3$ and the sodium salts **2** and **3**, respectively (Scheme 1). Several attempts to synthesize Ag(I) complexes with two PTA as coligands have been unsuccessful, even modifying the reaction conditions and stoichiometric ratio between the reagents. Analytical and spectroscopic data suggest the 1 : 1 : 1 stoichiometry for complexes **8** and **11**, with PTA coordinated *via* the phosphorus atom. On the other hand, PTA acts as a monodentate P-donor ligand in a vast majority of known complexes,[109] although in the absence of crystallography data we cannot exclude that the PTA binds the metal in the bridging *N*,*P*-coordination mode.[110]

The IR spectra recorded for the solid samples of **8** and **11** show all the expected bands for the β-diketone ligand and the 1,3,5-triazaphosphaadamantane co-ligands. The absorptions due to the C═O stretching are at 1513–1610 cm^{-1} and they don't significantly vary with respect to the same absorptions in the spectra of the free ligand salts. The ^{1}H-NMR spectra of complexes **8** and **11**, recorded in CD_3OD solution at room temperature, show a single set of resonances for the β-diketone moiety, indicating that the protons of the aromatic rings are equivalents, with a slight shift due to the coordination to the metal center. The PTA co-ligands show a characteristic series of peaks in the range of 4.15–4.67 ppm, with an

integration that confirms the 1 : 1 stoichiometry. The ESI-MS study was performed by dissolving **8** and **11** in CH_3OH. In the positive-ion mode spectra we observed at *m*/*z* 158 and 420 the presence of peaks attributable to the $[PTA + H]^+$ and $[Ag(PTA)_2]^+$ species, respectively, due to the dissociation of the ligand from the complexes.

It's interesting to note that the diagnostic COC*H*CO signal is at 6.17 and 6.21 ppm in the spectra recorded in $CDCl_3$ of $[Cu(L^{CF3})(PPh_3)_2]$ (**4**) and $[Ag(L^{CF3})(PPh_3)_2]$ (**5**), respectively, and the related peak is present at 6.57 ppm in the spectrum of sodium salt NaL^{CF3} (**1**) in DMSO-d_6 solution and at 6.91 in the spectrum of HL^{CF3} in $CDCl_3$ solution. In the $^{13}C\{^1H\}$-NMR spectra of **4** and **5** the COC*H*CO signals are at 92.02 and 92.35 ppm, respectively, and the related peaks are at 90.91 and 93.82 ppm in the spectra of the free ligands **1** and HL^{CF3}. In the ^1H-NMR spectra of $[Cu(L^{Mes})(PPh_3)_2]$ (**6**), $[Ag(L^{Mes})(PPh_3)_2]$ (**7**) and $[Ag(L^{Mes})(PTA)]$ (**8**), recorded in $CDCl_3$ or DMSO-d_6, the COC*H*CO signals are at 4.81–5.34, and the related peaks are present at 5.29 and 5.77 ppm in the spectra of NaL^{Mes} (**2**) and HL^{Mes}, respectively, in $CDCl_3$ solution. In the $^{13}C\{^1H\}$-NMR spectra of **6–8** the COC*H*CO signals are at 101.66–103.75, and the related peak is at 103.85 and 105.48 ppm, in the spectra of the free ligands **2** and HL^{Mes}. Finally, the COC*H*CO signals are at 6.40–6.78 ppm in the spectra recorded in $CDCl_3$ or CD_3OD for $[Cu(L^{Ph})(PPh_3)_2]$ (**9**), $[Ag(L^{Ph})(PPh_3)_2]$ (**10**) and $[Ag(L^{Ph})(PTA)]\cdot H_2O$ (**11**), respectively, and the related peaks are present at 6.87 and 6.89 ppm in the spectra of the sodium salt NaL^{Ph} (**3**) and HL^{Ph} in acetone-d_6 and $CDCl_3$ solution, respectively. In the $^{13}C\{^1H\}$-NMR spectra of **9–11** the COC*H*CO signals are at 90.35–93.38 ppm and the related peak is at 93.21 ppm in the spectrum of the free ligand **3**. In the $^{13}C\{^1H\}$-NMR spectra of **9–11** the COC*H*CO signals are at 90.35–93.38 ppm, and the related peaks are at 93.21 and 93.18 ppm, in the spectra of the free ligands **3** and HL^{Ph}.

The room temperature $^{31}P\{H\}$-NMR spectra of the Cu(I) complexes **4**, **6** and **9**, recorded in $CDCl_3$ or CD_2Cl_2 solution, exhibited single signals at −3.68, −5.41 and −3.96 ppm, respectively, downfield shifted with respect to the value of the free triphenylphosphine PPh_3 (δ = −4.85 ppm in $CDCl_3$ and −5.55 ppm in CD_2Cl_2). The room temperature $^{31}P\{H\}$-NMR spectra of the Ag(I) complexes, recorded in $CDCl_3$ solution (compounds **5**, **7**, and **10**) or CD_3OD solution (compounds **8** and **11**), gave singlet signals downfield shifted with respect to the value of the free phosphanes PPh_3 and PTA (δ = −4.85 and −102.07 ppm, respectively). At 223 K, the spectra of **5** and **7** (in the $CDCl_3$ solvent) show one pair of doublets in which the coupling of ^{31}P to the ^{107}Ag and ^{109}Ag is resolved, in accordance with a stopped or slow triphenylphosphane exchange process: the $^1J(^{107}Ag–^{31}P)$ and $^1J(^{109}Ag–^{31}P)$ coupling constants are respectively in the range of 408–430 and 472–496 Hz for compounds **5** and **7**, being of the same order of magnitude as those reported for analogous silver(I) bis(triphenylphosphine) species.[111–113] At 223 K, compound **10** exhibits a broad doublet with a $^1J(Ag–^{31}P)$ coupling constant of 439 Hz. The ratio of $^1J(^{109}Ag–^{31}P)/^1J(^{107}Ag–^{31}P)$ is in good agreement with the $^{107}Ag/^{109}Ag$ gyromagnetic ratio of 1.15. The room temperature $^{31}P\{H\}$-NMR spectra of complexes **8** and **11** with PTA coligands, recorded in CD_3OD solution, gave singlets centered at δ −83.73 and −83.82 ppm, while at 243 K they exhibited broad signals, centered at about −81 ppm, in which the coupling of ^{31}P to $^{107/109}Ag$ is not resolved.

Compounds $[Cu(L^{CF3})(PPh_3)_2]$ (**4**) and $[Ag(L^{Ph})(PPh_3)_2]$ (**10**) produced a crystalline material suitable for X-ray crystallography. They crystallize as discrete molecules in the space groups $P\bar{1}$ and $P2_1/n$, respectively, and the molecular structures are illustrated in Fig. 2 and 3. There are two chemically similar molecules in the asymmetric unit of $[Cu(L^{CF3})(PPh_3)_2]$. Both the copper and silver complexes adopt a distorted tetrahedral

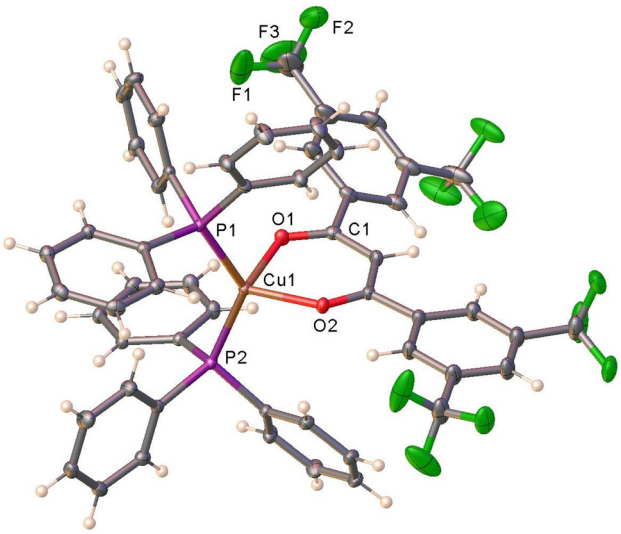

Fig. 2 Molecular structure of $[Cu(L^{CF3})(PPh_3)_2]$ (**4**) (only one of the two molecules present in the asymmetric unit is shown).

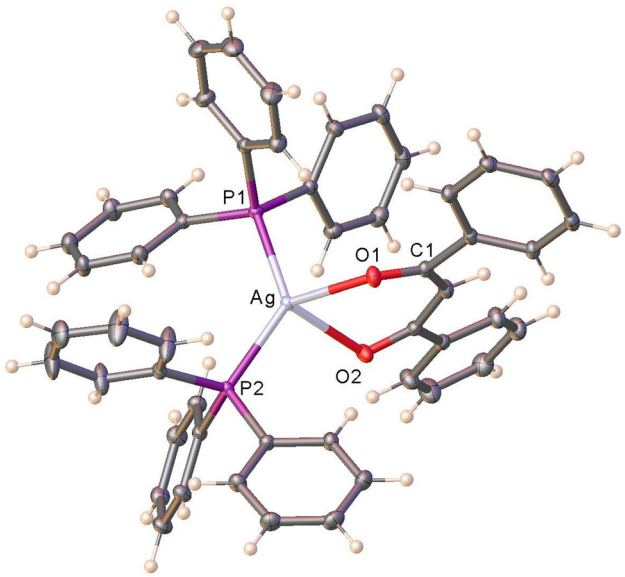

Fig. 3 Molecular structure of $[Ag(L^{Ph})(PPh_3)_2]$ (**10**).

geometry. Complete details of the bond distances and angles are given in the ESI.† Although the diketonate based CuO_2C_3 metallacycle is essentially planar in $[Cu(L^{CF3})(PPh_3)_2]$ (Fig. 2), the AgO_2C_3 core of the silver complex $[Ag(L^{Ph})(PPh_3)_2]$ (Fig. 3) adopts a half-boat conformation with the silver atom residing out of the O_2C_3 plane. The average Cu–P distance and Cu–O distances of $[Cu(L^{CF3})(PPh_3)_2]$ (2.2256 and 2.071 Å, respectively) are shorter than the Ag–P and Ag–O distances in $[Ag(L^{Ph})(PPh_3)_2]$ (average 2.424 and 2.343 Å, respectively), which is expected due to the larger covalent radius of silver relative to copper. The P–M–P angles (M = Cu, Ag) are very similar between the two systems (128.50° and 129.20° for **4** and **10**, respectively). A comparison of Cu–O distances of $[Cu(L^{CF3})(PPh_3)_2]$ (av. 2.071 Å) and $[Cu(L^{Ph})(PPh_3)_2]$ (av. 2.058 Å) indicates that the latter featuring more electron donating β-diketonate has slightly shorter Cu–O contacts.[51] The Cu–P distances of these two molecules (av. 2.2256 Å of $[Cu(L^{CF3})(PPh_3)_2]$ and av. 2.250 Å of $[Cu(L^{Ph})(PPh_3)_2]$) show an opposite trend. We have also confirmed the identity of $[Cu(L^{Mes})(PPh_3)_2]$ (**6**) using X-ray crystallography. It is also a four-coordinate, pseudo-tetrahedral complex (see the ESI, Fig. S2†). Unfortunately, the weakly diffracting sample and crystal twinning of $[Cu(L^{Mes})(PPh_3)_2]$ prevented us from obtaining high quality data suitable for detailed analysis of structural features.

Biological studies

The stability of the new complexes in 0.5% DMSO/physiological solution was evaluated by UV-Vis spectroscopy. Spectra were recorded every 24 h in the range of 240–640 nm over 72 h. The collected spectra for all complexes are reported in the ESI, Fig. S3† showing that all compounds were sufficiently stable under physiological conditions. All the spectra, and in particular the spectra registered for complexes **4** and **10** showed curves with a progressive increase in the baseline adsorption, probably due to solubility issues.

The Ag(I) and Cu(I) complexes and the corresponding uncoordinated ligands and their salts were evaluated for their cytotoxic activity towards various human cancer cell lines representative of different solid tumors. Cytotoxicity of PPh_3 and PTA ligands have already been published.[114] In particular, the in-house cancer cell panel contained examples of human colon (HCT-15), pancreatic (PSN-1 and BxPC3), testicular (NTERA-2), and breast (MDA-MB-231), as well as SCLC (U1285) and NSCLC (A549). The cytotoxicity parameters, expressed in terms of IC_{50} values obtained after 72 h of exposure to the MTT assay, are reported in Table 1. For comparison, the cytotoxicity of the reference metal-based chemotherapeutic drug cisplatin was assessed under the same experimental conditions.

NaL^{Ph}/HL^{Ph} and NaL^{CF3}/HL^{CF3} ligands proved to be hardly effective against all tested cancer cell lines. In contrast, NaL^{Mes}/HL^{Mes} ligands were quite effective in inhibiting cancer cell growth, with IC_{50} values in the low micromolar range. It is interesting to note that in the case of PPh_3-containing Cu(I) and Ag(I) complexes, metal coordination significantly improved the cytotoxic potency compared to the free ligand, conversely, for $[Ag(L^{Mes})(PTA)]$ sensibly higher IC_{50} values were always obtained, confirming that the bioactivity of the metal complex depends on the full set of coordinating ligands. All tested complexes demonstrated a marked cytotoxic activity towards cancer cell lines belonging to the in-house cancer cell panel, showing IC_{50} values in the low/sub micromolar range. On average, the PPh_3 derivatives were more effective than cisplatin, whereas the two Ag(I) complexes bearing the PTA moiety were less effective than the reference metallodrug cisplatin. Among the PPh_3 derivatives, Cu and Ag complexes bearing the L^{Mes} ligand were the most effective derivatives, with average IC_{50} values of 2.4 and 4.0 μM, respectively. It is noteworthy that against testicular carcinoma NTERA-2 cells,

Table 1 2D cytotoxicity

IC_{50} (μM) ± S.D.

	NTERA-2	HCT-15	BxPC3	U-1285	PSN-1	A549	MDA-MB-231
HL^{CF3}	21.1 ± 0.9	43.5 ± 8.2	>50	44.8 ± 5.8	>50	>50	>50
NaL^{CF3}	ND	ND	ND	ND	ND	ND	ND
$[Cu(L^{CF3})(PPh_3)_2]$	1.3 ± 0.4	2.0 ± 0.5	1.2 ± 0.4	1.5 ± 0.5	4.4 ± 0.3	5.4 ± 0.9	5.3 ± 1.2
$[Ag(L^{CF3})(PPh_3)_2]$	3.5 ± 0.6	2.1 ± 0.4	2.9 ± 0.1	2.6 ± 0.2	6.3 ± 1.2	11.1 ± 1.5	11.3 ± 2.2
HL^{Mes}	3.6 ± 0.1	5.3 ± 0.7	7.5 ± 1.2	8.1 ± 1.1	5.2 ± 0.8	12.5 ± 3.6	ND
NaL^{Mes}	5.7 ± 0.8	4.6 ± 1.4	4.3 ± 0.9	5.1 ± 0.5	4.1 ± 0.3	9.1 ± 2.3	ND
$[Cu(L^{Mes})(PPh_3)_2]$	0.9 ± 0.3	1.2 ± 0.5	1.1 ± 0.4	1.2 ± 0.7	1.3 ± 0.5	5.6 ± 1.1	5.5 ± 0.8
$[Ag(L^{Mes})(PPh_3)_2]$	1.7 ± 0.6	2.5 ± 1.0	1.7 ± 0.5	2.7 ± 0.9	2.1 ± 0.7	7.6 ± 1.4	9.5 ± 2.3
$[Ag(L^{Mes})(PTA)]$	12.8± 2.5	19.5 ± 3.1	14.9 ± 2.2	17.3 ± 2.7	15.7 ± 1.9	22.8 ± 3.3	28.1 ± 3.4
HL^{Ph}	>50	>50	>50	39.5 ± 2.8	38.5 ± 4.1	>50	>50
NaL^{Ph}	29.7 ± 5.4	25.2 ± 2.9	27.5 ± 0.1	29.2 ± 3.4	28.8 ± 4.1	>50	>50
$[Cu(L^{Ph})(PPh_3)_2]$	5.1 ± 0.6	8.5 ± 1.5	6.2 ± 0.8	12.3 ± 2.2	9.8 ± 2.1	15.2 ± 2.8	25.3 ± 3.1
$[Ag(L^{Ph})(PPh_3)_2]$	3.0 ± 0.4	1.9 ± 0.8	3.1 ± 0.8	4.2 ± 1.1	2.4 ± 0.1	8.3 ± 1.9	9.1 ± 2.1
$[Ag(L^{Ph})(PTA)]$	35.8 ± 5.8	37.2 ± 2.5	40.7 ± 2.9	28.6 ± 4.1	25.3 ± 4.2	>50	>50
Cisplatin	14.6 ± 3.0	13.9 ± 1.6	11.9 ± 1.3	2.1 ± 0.8	12.1 ± 2.8	9.1 ± 1.4	21.5 ± 4.1

Cells (3–8 × 10^3 cells per well) were treated for 72 h with increasing concentrations of tested compounds. Cytotoxicity was assessed by the MTT test. The IC_{50} values were calculated by the four-parameter logistic model ($p < 0.05$).

Table 2 3D cytotoxicity

IC_{50} (μM) ± S.D.	HCT-15
$[Cu(L^{CF3})(PPh_3)_2]$	58.5 ± 5.8
$[Ag(L^{CF3})(PPh_3)_2]$	>100
$[Cu(L^{Mes})(PPh_3)_2]$	86.6 ± 6.7
$[Ag(L^{Mes})(PPh_3)_2]$	>100
$[Ag(L^{Mes})(PTA)]$	>100
$[Cu(L^{Ph})(PPh_3)_2]$	>100
$[Ag(L^{Ph})(PPh_3)_2]$	82.5 ± 5.8
$[Ag(L^{Ph})(PTA)]$	>100
Cisplatin	59.5 ± 3.3

Cells (2.5×10^3 cells per well) were treated for 72 h with increasing concentrations of tested compounds. Cytotoxicity was assessed by the APH assay. The IC_{50} values were calculated using the four-parameter logistic model ($p < 0.05$).

$[Cu(L^{Mes})(PPh_3)_2]$ was up to 16-fold more efficacious than cisplatin in decreasing cell proliferation. Conversely, the weakest PPh_3 derivatives were those bearing the L^{Ph} ligand. Interestingly, Cu(I) complexes containing the L^{CF3} and L^{Mes} ligands were much more effective (about 2-fold) than the corresponding Ag(I) derivatives whereas in the case of the L^{Ph} ligand, the Ag(I) complex was about 2.7 times more effective than the corresponding copper derivative.

The *in vitro* antitumor activity of the newly developed Cu(I) and Ag(I) derivatives was also assayed in 3D cell culture models of human colon cancer cells. Although the two-dimensional cell cultures are the most employed assays for *in vitro* screening (due to the low cost, simplicity, and reliability), 2D methods are unable to mimic the *in vivo* properties of solid tumor models. On the other hand, 3D cell cultures are much more effective in closely mimicking the heterogeneity and complexity of the tumor mass, and therefore are more predictive for *in vivo* results than conventional 2D cell cultures.[115] On these bases, we tested the activity of the newly developed complexes on spheroids obtained from human HCT-15 tumor cells. HCT15 cells are known for their ability to form spheroids, which makes them a valuable tool for studying the interactions between cancer cells and the surrounding microenvironment. Human colon cancer cell spheroids were treated with the investigated compounds for 72 h, and cell viability was assessed by means of the acid phosphatase (APH) assay and the results are reported in Table 2. Results, reported in Table 2, were completely different from those obtained by 2D screening, and clearly showed that among the new Cu(I) and Ag(I) complexes, only derivative $[Cu(L^{CF3})(PPh_3)_2]$ possessed an antiproliferative activity against 3D tumor spheroids comparable to that of the reference drug cisplatin.

Conclusions

In this study, we report the synthesis, characterization and biological evaluation of Cu(I) and Ag(I) phosphane complexes supported by the anion of sterically hindered β-diketone ligands. In particular, 1,3-dimesitylpropane-1,3-dione (HL^{Mes}) and 1,3-bis(3,5-bis(trifluoromethyl)phenyl)-3-hydroxyprop-2-en-1-one (HL^{CF3}) characterized by the presence of trifluoromethyl or methyl groups on the phenyl moieties were employed for the preparation of the complexes **4–11**, using the lipophilic PPh_3 and the hydrophilic PTA as co-ligands to stabilize the metal in the +1 oxidation state. The analogous complexes of the anion of the parent 1,3-diphenylpropane-1,3-dione (HL^{Ph}) ligand were also synthesized and evaluated for their antitumor activity to compare the biological effects of substituents on the phenyl moieties.

The compounds were fully characterized both in the solid state and in solution. The X-ray crystal structures of $[Cu(L^{CF3})(PPh_3)_2]$ and $[Ag(L^{Ph})(PPh_3)_2]$ show that both the copper and silver complexes adopt a distorted tetrahedral geometry. The diketonate based CuO_2C_3 metallacycle is essentially planar in $[Cu(L^{CF3})(PPh_3)_2]$, while the AgO_2C_3 core of $[Ag(L^{Ph})(PPh_3)_2]$ adopts a half-boat conformation with the silver atom residing out of the O_2C_3 plane.

Biological studies highlighted that both Ag(I) and Cu(I) complexes containing PPh_3 as the phosphane coligand were more potent than cisplatin in inhibiting cancer cell growth. Among them, Cu complexes bearing the L^{CF3} and L^{Mes} ligands were the most effective derivatives, in particular $[Cu(L^{Mes})(PPh_3)_2]$ was up to 16-fold more efficacious than cisplatin in decreasing the cell proliferation of 2D testicular carcinoma cell cultures. Cytotoxicity experiments performed exploiting the proclivity of HCT-15 cells to form spheroids showed that $[Cu(L^{CF3})(PPh_3)_2]$ possessed a marked antiproliferative activity against 3D tumor spheroids, confirming the ability of this derivative to penetrate across the entire spheroid domain and reach the inner hypoxic core.

Experimental section

Chemistry

Materials and general methods. All the reagents were obtained from commercial sources and used as received. Melting points (MP) were performed on an Stuart Scientific SMP3 instrument (Bibby Sterilin Ltd, London, UK). Elemental analyses (C, H, N) (EA) were performed with a Fisons Instruments EA-1108 CHNS-O Elemental Analyzer (Thermo Fisher Scientific Inc., Waltham, MA, USA). Fourier transform infrared (FT-IR) spectra were recorded from 4000 to 700 cm^{-1} on a PerkinElmer Frontier Instrument (PerkinElmer Inc., Waltham, MA, USA), equipped with an attenuated total reflection (ATR) unit using universal diamond top-plate as the sample holder. Abbreviations used in the analyses of the FT-IR spectra are as follows: br = broad, m = medium, mbr = medium broad, s = strong, sbr = strong broad, vs = very strong, w = weak, and wbr = weak broad. Nuclear magnetic resonance (NMR) spectra for the ^1H, ^{13}C and ^{31}P nuclei were recorded with a Bruker 500 Ascend spectrometer (Bruker BioSpin Corporation, Billerica, MA, USA; 500.13 MHz for ^1H, 125.78 MHz for ^{13}C, 202.46 MHz for ^{31}P and 470.59 MHz for

^{19}F). Tetramethylsilane ($SiMe_4$) was used as the external standard for the ^{1}H- and ^{13}C-NMR spectra, while 85% H_3PO_4 was used for the ^{31}P-NMR spectra. The chemical shifts (δ) are reported in ppm, and coupling constants (J) are reported in hertz (Hz). Abbreviations used in the analyses of the NMR spectra are as follows: br = broad, d = doublet, m = multiplet, s = singlet, sbr = singlet broad, and t = triplet. ElectroSpray ionization mass spectra (ESI-MS) were recorded in positive-(ESI-MS(+)) or negative-ions (ESI-MS(−)) modes on a Waters Micromass ZQ Spectrometer equipped with a single quadrupole (Waters Corporation, Milford, MA, USA), using the methanol or acetonitrile mobile phase. The compounds were added to reagent grade methanol or acetonitrile to give approximately 0.1 mM solutions. These solutions were injected (1 μL) into the spectrometer fitted with an autosampler. The pump delivered the solutions to the mass spectrometer source at a flow rate of 200 μL min^{-1} and nitrogen was employed both as a drying and nebulizing gas. The capillary voltage was typically 2500 V. The temperature of the source was 100 °C, while the temperature of desolvation was 400 °C. In the analyses of ESI-MS spectra, the confirmation of major peaks was supported by the comparison of the observed and predicted isotope distribution patterns, the latter were calculated using the IsoPro 3.1 computer software (T-Tech Inc., Norcross, GA, USA).

*NaL^{CF3} (**1**).* The ligand HL^{CF3} (3.000 mmol, 1.489 g) and NaOH (3.000 mmol, 0.120 g) were dissolved in ethanol (100 mL), obtaining an opalescent yellow solution. The reaction mixture was stirred at room temperature for 4 hours. The solution was then dried at reduced pressure giving the orange solid product NaL^{CF3} in 85% yield. M.p.: 226–230 °C. FT-IR (cm^{-1}, Fig. S4†): 3099wbr (C–H); 1628m, 1592m (C═O); 1580sh, 1511m, 1471m, 1421m, 1360s, 1275s, 1240m, 1189m; 1163s, 1121vs (CF_3); 1044m, 955m, 905s, 887m, 845m, 787s, 702m, 681s. ^{1}H-NMR (DMSO-d_6, 293 K, Fig. S5†): δ 6.57 (s, 1H, COC*H*CO), 8.08 (s, 2H, *p*-CH_{ar}), 8.48 (s, 4H, *o*-CH_{ar}). ^{13}C{^{1}H}-NMR (DMSO-d_6, 293 K, Fig. S6†): δ 90.91 (CO*C*HCO); 123.96 (q, $^{1}J_{CF}$ = 273 Hz, *C*F_3); 130.40 (q, $^{2}J_{CF}$ = 33 Hz, *C*CF_3); 122.88, 127.68, 146.16 (*C*H_{ar} and *C*$_{ar}$); 179.21 (*C*O). ^{19}F{^{1}H}-NMR (DMSO-d_6, 293 K, Fig. S7†): δ −61.21 (s). ESI-MS (major positive ions, CH_3CN), *m*/*z* (%): 541 (40) $[NaL^{CF3} + Na]^+$. Elemental analysis calculated for $C_{19}H_7F_{12}NaO_2$: C 44.04, H 1.36; found: C 43.89, H 1.34.

*NaL^{Mes} (**2**).* To the ligand HL^{Mes} (2.00 mmol, 0.617 g) solubilized in methanol (15 mL), NaOH (2.000 mmol, 0.080 g) was added. The reaction mixture was stirred under reflux for 24 hours. The solution was dried at reduced pressure and the residue was recrystallized by diethyl ether and filtered. From the mother liquors, dried at reduced pressure, the light orange whitish compound NaL^{Mes} has been obtained in 74% yield. M.p.: 102–104 °C. FT-IR (cm^{-1}, Fig. S8†): 3281wbr, 3147wbr, 2971wbr, 2951wbr, 2918w, 2858w (C–H); 1611m, 1565br (C═O); 1557m, 1499m, 1417sbr, 1373s, 1298w, 1271m, 1164m, 1110m, 1028mbr, 955w, 926w, 882w, 848m, 791m, 779m, 718m. ^{1}H-NMR ($CDCl_3$, 293 K, Fig. S9†): δ 2.23 (s, 6H, *p*-CH_3), 2.24 (s, 12H, *o*-CH_3), 5.29 (s, 1H, COC*H*CO), 6.72 (s, 4H, *m*-C*H*). ^{13}C{^{1}H}-NMR ($CDCl_3$, 293 K, Fig. S10†): δ 19.58 (*o*-*C*CH_3); 20.96 (*p*-*C*CH_3); 103.85 (CO*C*HCO); 127.85, 132.65, 133.20, 136.10 (*C*H_{ar} and *C*$_{ar}$); 191.24 (*C*O). ESI-MS(+) (major positive ions, CH_3OH), *m*/*z* (%): 331 (100) $[NaL^{Mes} + H]^+$, 353 (40) $[NaL^{Mes} + Na]^+$, 683 (10) $[2NaL^{Mes} + Na]^+$. ESI-MS(−) (major negative ions, CH_3OH), *m*/*z* (%): 307 (100) $[L^{Mes}]^-$, 637 (10) $[2L^{Mes} + Na]^-$. Elemental analysis (%) calculated for $C_{21}H_{23}NaO_2$: C 76.32, H 7.02; found C 74.09, H 7.09.

*NaL^{Ph} (**3**).* The ligand HL^{Ph} (10.000 mmol, 2.243 g) and NaOH (10.000 mmol, 0.400 g) were solubilized in methanol (60 mL) and the reaction was stirred at room temperature for 24 hours under constant magnetic stirring. The precipitate formed was filtered and the mother liquors were evaporated at reduced pressure. The white product NaL^{Ph} was obtained in 80% yield. M.p.: 300–304 °C. FT-IR (cm^{-1}, Fig. S11†): 3302wbr, 3160wbr, 3058w, 2939wbr, 2827wbr; 1643w, 1596s (C═O); 1556vs, 1510s, 1452vs, 1426vs, 1383s, 1297s, 1276s, 1219s, 1176m, 1114m, 1072m, 1044s, 1012s, 999m, 946m, 937m, 851w, 814w, 785s, 767s, 730vs. ^{1}H-NMR (CD_3OD, 293 K, Fig. S12†): δ 7.39–7.40 (m, 6H, CH_{ar}), 7.84–7.85 (m, 4H, CH_{ar}). ^{1}H-NMR (acetone-d_6, 293 K, Fig. S13†): δ 6.51 (s, 1H, COC*H*CO), 7.31–7.37 (m, 6H, CH_{ar}), 7.92–7.94 (m, 4H, CH_{ar}). ^{13}C{^{1}H}-NMR (acetone-d_6, 293 K, Fig. S14†): δ 91.47 (CO*C*HCO); 126.92, 127.69, 129.04, 143.6 (*C*H_{ar} and *C*$_{ar}$); 183.64 (*C*O). ESI-MS(+) (major positive ions, EtOH), *m*/*z* (%): 247 (100) $[NaL^{Ph} + H]^+$. Elemental analysis calculated for $C_{15}H_{11}NaO_2$: C 73.17, H 4.50; found: C 72.51, H 4.54.

*$[Cu(L^{CF3})(PPh_3)_2]$ (**4**).* Tetrakis(acetonitrile)copper(I) hexafluorophosphate (0.500 mmol, 0.186 g) and triphenylphosphine (1.000 mmol, 0.262 g,) were solubilized in CH_3CN (40 mL). The reaction mixture was kept under constant magnetic stirring at room temperature overnight. Then, ligand NaL^{CF3} (0.500 mmol, 0.259 g,) was added to the solution. After 5 hours of stirring, the mixture was evaporated and the solid formed was washed in Et_2O. From the mother liquors an orange solid was precipitated, and it was crystallized using Et_2O and *n*-hexane to give complex **4** in 60% yield. A batch of good quality crystals of $Cu(L^{CF3})(PPh_3)_2$, suitable for X-ray analysis, was obtained by slow evaporation of an ethanol/acetone solution of **4**. M.p.: 109–112 °C. FT-IR (cm^{-1}, Fig. S15†): 3056wbr (C–H); 1626w, 1582m (C═O); 1539w, 1519w, 1501w, 1480s, 1435m, 1417m, 1360s, 1275vs, 1247m; 1171s, 1125vs (CF_3); 1097s, 1027m, 998w, 952m, 903m, 844m, 790w, 778m, 744s, 693s, 680s, 663m. ^{1}H-NMR ($CDCl_3$, 293 K, Fig. S16†): δ 6.17 (s, 1H, COC*H*CO), 7.22–7.41 (m, 30H, CH_{ar}), 7.90 (s, 2H, *p*-CH_{ar}), 8.11 (s, 4H, *o*-CH_{ar}). ^{1}H-NMR (DMSO-d_6, 293 K, Fig. S17†): δ 6.72 (s, 1H, COC*H*CO), 7.31–7.65 (m, 30H, CH_{ar}), 8.19 (s, 2H, *p*-CH_{ar}), 8.38 (s, 4H, *o*-CH_{ar}). ^{13}C{^{1}H}-NMR ($CDCl_3$, 293 K, Fig. S18†): δ 92.03 (CO*C*HCO); 123.42 (q, $^{1}J_{CF}$ = 273 Hz, *C*F_3); 131.23 (q, $^{2}J_{CF}$ = 33 Hz, *C*CF_3); 123.09, 126.95, 128.43, 129.58, 133.41, 133.60, 133.79, 133.88, 144.36 (*C*H_{ar} and *C*$_{ar}$); 181.65 (*C*O). ^{31}P{^{1}H}-NMR ($CDCl_3$, 223 K, Fig. S19†): δ −3.68 (s). ESI-MS (major positive ions, CH_3CN), *m*/*z* (%): 366 (40) $[Cu(PPh_3) + CH_3CN]^+$, 587 (100) $[Cu(PPh_3)_2]^+$. ^{19}F{^{1}H}-NMR ($CDCl_3$, 293 K, Fig. S20†): δ −62.64 (s). ESI-MS (major negative ions, CH_3CN), *m*/*z* (%): 495 (100) $[L^{CF3}]^-$. Elemental analysis

(%) calculated for $C_{55}H_{37}CuF_{12}O_2P_2$: C 60.98, H 3.44; found: C 59.95, H 3.36.

*[Ag(L^{CF3})(PPh_3)$_2$] (**5**).* Silver nitrate (0.500 mmol, 0.085 g,) and PPh_3 (1.000 mmol, 0.262 g) were solubilized in a methanol/acetonitrile solution (20/20 mL). The reaction mixture was stirred for 3 hours at room temperature in the dark. Subsequently, the HL^{CF3} ligand (0.500 mmol, 0.248 g) was added and after 1 hour NaOH (0.500 mmol, 0.020 g) was added to the reaction solution. The reaction was run for 3 hours at room temperature in the dark. The yellow opalescent precipitate was filtered off; the solution was evaporated to dryness and the yellow solid product was solubilized in diethyl ether, and purified by filtration to give compound **5** in 40% yield. M.p.: 140–143 °C. FT-IR (cm^{-1}, Fig. S21†): 3056wbr, 2985wbr, 2855wbr (CH); 1626m, 1591m (C═O); 1524w, 1504w, 1504w, 1471m, 1456sh, 1446w, 1434m, 1425m, 1361s, 1327w, 1276vs, 1232sh, 1220m; 1168s, 1123vs (CF_3); 1095sh, 1027m, 997m, 972w, 949m, 940sh, 924m, 902m, 845m, 794m, 778m, 742s, 704sh, 692vs, 683vs. ^{1}H-NMR ($CDCl_3$, 293 K, Fig. S22†): δ 6.21 (s, 1H, COC*H*CO), 7.27–7.50 (m, 30H, CH_{ar}), 7.94 (s, 2H, *p*-CH_{ar}), 8.23 (s, 4H, *o*-CH_{ar}). ^{1}H-NMR (DMSO-d_6, 293 K, Fig. S23†): δ 6.88 (s, 1H, COC*H*CO), 7.37–7.50 (m, 30H, CH_{ar}), 8.23 (s, 2H, *p*-CH_{ar}), 8.51 (s, 4H, *o*-CH_{ar}).^{13}C{^{1}H}-NMR ($CDCl_3$, 293 K, Fig. S24†): δ 92.35 (CO*C*HCO); 123.38 (q, $^1J_{CF}$ = 273 Hz, *C*F_3); 123.42, 127.13, 128.66, 128.74, 130.08, 131.33, 132.56, 132.77, 133.91, 134.04, 144.84 (*C*CF_3, *C*H_{ar} and C_{ar}); 182.48 (*C*O). ^{31}P{^{1}H}-NMR ($CDCl_3$, 293 K, Fig. S25†): δ 8.88 (s). ^{31}P{^{1}H}-NMR ($CDCl_3$, 223 K, Fig. S26†): δ 8.53 (d, $^1J(^{107}Ag–^{31}P)$ = 430 Hz and d, $^1J(^{109}Ag–^{31}P)$ = 496 Hz). ^{19}F{^{1}H}-NMR ($CDCl_3$, 223 K, Fig. S27†): δ −62.66 (s). ESI-MS(+) (major positive ions, CH_3CN), *m*/*z* (%): 633 (100) $[Ag(PPh_3)_2]^+$. ESI-MS(−) (major negative ions, CH_3CN), *m*/*z* (%): 495 (100) $[L^{CF3}]^-$. Elemental analysis (%) calculated for $C_{55}H_{37}AgF_{12}O_2$: C 58.58, H 3.31; found: C 57.61, H 3.49.

*[Cu(L^{Mes})(PPh_3)$_2$] (**6**).* Triphenylphospine (1.000 mmol, 0.262 g) and tetrakis(acetonitrile)copper(I) hexafluorophosphate (0.500 mmol, 0.186 g) were solubilized in a mixture of CH_2Cl_2/CH_3OH (15 : 5 mL). The colourless clear solution was stirred at room temperature for 1 hour. Successively, the ligand NaL^{Mes} (0.500 mmol, 0.165 g) was added and the green-yellow solution was stirred at room temperature for 3 hours. The mixture was then dried at reduced pressure giving a light green solid product. The product was washed firstly in Et_2O and in a second step in CH_3OH, giving a light green precipitate that was filtered and dried under reduced pressure. The light green complex **6** was obtained in 86% yield. A batch of poor quality crystals of [Cu(L^{Mes})(PPh_3)$_2$], suitable for X-ray analysis, was obtained by slow evaporation of a CH_2Cl_2 solution of **6**. M.p.: 210–215 °C. FT-IR (cm^{-1}, Fig. S28†): 3050wbr, 2953wbr, 2917wbr, 2855wbr (C–H); 1613w, 1555s (C═O); 1504m, 1479m, 1434s, 1395vs, 1372s, 1311m, 1281m, 1185w, 1167m, 1113m, 1093s, 1071m, 1027m, 997m, 956w, 924w, 849s, 880m, 777m, 742s, 724m, 693vs, 608m, 541m, 525s, 503vs. ^{1}H-NMR ($CDCl_3$, 293 K, Fig. S29†): δ 2.13–2.34 (s, 18H, *o*- and *p*-CH_3), 5.34 (s, 1H, COC*H*CO), 6.74 (s, 4H, *m*-CH_{ar}), 7.21–7.39 (m, 30H, CH_{ar}). ^{1}H-NMR (DMSO-d_6, 293 K, Fig. S30†): δ 2.05–2.16 (s, 18H, *o*- and *p*-CH_3), 5.05 (s, 1H, COC*H*CO), 6.71 (s, 4H, *m*-CH_{ar}), 7.28–7.63 (m, 30H, CH_{ar}). ^{13}C{^{1}H}-NMR ($CDCl_3$, 293 K, Fig. S31†): δ 19.72 (*o*-*C*CH_3); 20.96 (*p*-*C*CH_3); 103.75 (CO*C*HCO); 127.98, 128.49, 129.36, 131.93, 132.17, 133.92, 134.04, 136.11, 141.64 (*C*H_{ar} and C_{ar}); 189.37 (*C*O). ^{31}P{^{1}H}-NMR (CD_2Cl_2, 293 K, Fig. S32†): δ −5.41 (sbr). ESI-MS (+) (major positive ions, CH_2Cl_2/CH_3CN) *m*/*z* (%): 587 (100) $[Cu(PPh_3)_2]^+$. ESI-MS (−) (major negative ions, CH_2Cl_2/CH_3CN) *m*/*z* (%): 307 (100) $[L^{Mes}]^-$, 341 (100) $[L^{Mes} + Cl]^-$, 396 (65) $[Cu(PPh_3) + 2Cl]^-$. Elemental analysis calculated for $C_{57}H_{53}CuO_2P_2$: C 76.45, H 5.97; found: C 75.97, H 5.88.

*[Ag(L^{Mes})(PPh_3)$_2$] (**7**).* Silver nitrate (0.500 mmol, 0.085 g) was added to a methanol solution (20 mL) of triphenylphosphine (1.000 mmol, 0.262 g). The reaction mixture was stirred at room temperature and in the dark for one hour. Successively, the ligand NaL^{Mes} (0.500 mmol, 0.165 g) was added, and the reaction was left under constant magnetic stirring at room temperature for 4 hours. The precipitate formed was filtered and dried under reduced pressure to give whitish complex **7** in a 40% yield. M.p.: 194–198 °C. FT-IR (cm^{-1}, Fig. S33†): 3054wbr, 2989wbr, 2953wbr, 2915wbr, 2851wbr (C–H); 1612w, 1582m, 1557m (C═O); 1492m, 1479m, 1435m, 1397s, 1372m, 1266m, 1182w, 1166w, 1111w, 1096s, 1071w, 1027m, 996w, 846m, 787w, 743s, 722m. ^{1}H-NMR ($CDCl_3$, 293 K, Fig. S34†): δ 2.22 (s, 18H, *o*- and *p*-CH_3), 5.26 (s, 1H, COC*H*CO), 6.73 (s, 4H, *m*-CH_{ar}), 7.29–7.45 (m, 30H, CH_{ar}). ^{1}H-NMR (DMSO-d_6, 293 K, Fig. S35†): δ 2.19 (s, 18H, *o*- and *p*-CH_3), 5.45 (s, 1H, COC*H*CO), 6.73 (s, 4H, *m*-CH_{ar}), 7.41–7.46 (m, 30H, CH_{ar}). ^{13}C{^{1}H}-NMR ($CDCl_3$, 293 K, Fig. S36†): δ 19.57 (*o*-*C*CH_3); 20.98, 21.11 (*p*-*C*CH_3); 102.76 (CO*C*HCO); 127.88, 128.46, 128.55, 128.71, 128.78, 129.87, 132.08, 132.16, 132.99, 133.18, 133.27, 133.97, 134.10, 135.67, 142.72 (*C*H_{ar} and C_{ar}); 190.51 (*C*O). ^{31}P{^{1}H}-NMR ($CDCl_3$, 293 K, Fig. S37†): δ 6.73 (s). ^{31}P{^{1}H}-NMR ($CDCl_3$, 223 K, Fig. S38†): δ 6.22 (d, $^1J(^{107}Ag–^{31}P)$ = 408 Hz, and d, $^1J(^{109}Ag–^{31}P)$ = 472 Hz). ESI-MS(+) (major positive ions, CH_3OH), *m*/*z* (%): 633 (100) $[Ag(PPh_3)_2]^+$. Elemental analysis calculated for $C_{57}H_{53}AgO_2P_2$: C 74.84, H 5.68; found: C 73.91, H 5.62.

*[Ag(L^{Mes})(PTA)] (**8**).* To a methanol (30 mL) solution of 1,3,5-triazaphosphaadamantane (2.000 mmol, 0.314 g), $AgNO_3$ (1.000 mmol, 0.170 g) was added, and the solution was stirred at room temperature in the dark for 2 hours. Successively, the ligand NaL^{Mes} was added (1000 mmol, 0.330 g) and the reaction mixture was left under magnetic stirring in the dark for 4 hours. The mixture was then filtered, and the precipitate was dried under reduced pressure, obtaining the orange complex **8** in 51% yield. M.p.: 193–197 °C. FT-IR (cm^{-1}, Fig. S39†): 3176wbr, 2948wbr, 2917wbr, 2861wbr (C–H); 1610m, 1574mbr, 1558mbr (C═O); 1497m, 1418sbr, 1373s, 1351s, 1286mbr, 1241m, 1164m, 1104m, 1039m, 1013m, 972s, 949m, 902wbr, 849m, 827mbr, 792m, 746m, 718s. ^{1}H-NMR (CD_3OD, 293 K, Fig. S40†): δ 2.24 (s, 6H, *p*-CCH_3), 2.32 (s, 12H, *o*-CCH_3), 4.28 (d, 6H, PCH_2N), 4.01–4.93 (m, 6H, NCH_2N), 6.79 (s, 4H, *m*-CH_{ar}).^{1}H-NMR (DMSO-d_6, 293 K, Fig. S41†): δ 2.18–2.28 (d, 18H, *p*- and *o*-CCH_3), 4.15 (s, 6H, PCH_2N), 4.41–4.57 (m, 6H, NCH_2N), 4.81 (s, 1H, COC*H*CO), 6.72 (s, 4H, *m*-CH_{ar}). ^{13}C{^{1}H}-

NMR (DMSO-d_6, 293 K, Fig. S42†): δ 19.69, 21.06 (*C*H_3); 51.06 (P*C*H_2N); 72.68, 72.73 (NC*H*$_2$N); 101.66 (COC*H*CO), 127.88, 132.87 (*C*H_{ar} and C_{ar}), 188.37 (*C*O). $^{31}P\{^1H\}$-NMR (CD_3OD, 293 K, Fig. S43†): δ −83.73 (s). $^{31}P\{^1H\}$-NMR (D_2O, 293 K, Fig. S44†): δ −81.50 (s). $^{31}P\{^1H\}$-NMR (CD_3OD, 223 K, Fig. S45†): δ −81.2 (br). ESI-MS(+) (major positive ions, CH_3OH), *m*/*z* (%): 158 (100) $[PTA + H]^+$, 420 (36) $[Ag(PTA)_2]^+$. Elemental analysis (%) calculated for $C_{27}H_{35}AgN_3O_2P$: N 7.34, C 56.65, H 6.16; found: N 6.95, C 55.66, H 6.03.

*[Cu(L^{Ph})(PPh$_3$)$_2$] (**9**).* Triphenylphosphine (2.000 mmol, 0.524 g) was solubilized in CH_2Cl_2 (25 mL) and copper(I) chloride (1.000 mmol, 0.099 g) was added. The solution was stirred for 3 hours at room temperature. Successively, ligand NaL^{Ph} (1.000 mmol, 0.246 g) was added, and the reaction was left under constant magnetic stirring for 2 hours. The mixture was filtered, and the mother liquors were evaporated at reduced pressure. The residue was washed in EtOH, filtered and dried at reduced pressure. The yellow complex **9** was obtained in 34% yield. M.p.: 209–213 °C. FT-IR (cm^{-1}, Fig. S46†): 3072w, 3046wbr, 3003w (C–H); 1596m, 1548s (C=O); 1511s, 1477m, 1455s, 1434s, 1403sbr, 1304m, 1273m, 1222m, 1179m, 1160m, 1092m, 1068m, 1022m, 997m, 936m, 922mbr, 840w, 806w, 784m, 741s, 719s. ^{1}H-NMR ($CDCl_3$, 293 K, Fig. S47†): δ 6.40 (s, 1H, COC*H*CO), 7.24–7.44 (m, 36H, C*H*$_{ar}$), 7.79 (d, 4H, C*H*$_{ar}$). ^{1}H-NMR (DMSO-d_6, 293 K, Fig. S48†): δ 6.47 (s, 1H, COC*H*CO), 7.29–7.42 (m, 36H, C*H*$_{ar}$), 7.83 (d, 4H, C*H*$_{ar}$). $^{13}C\{^1H\}$-NMR ($CDCl_3$, 293 K, Fig. S49†): δ 93.06 (CO*C*HCO); 126.91, 127.80, 128.35, 128.42, 128.46, 128.55, 129.32, 132.08, 132.16, 133.93, 134.05, 134.14 (*C*H_{ar} and C_{ar}); 184.59 (*C*O). $^{31}P\{^1H\}$-NMR ($CDCl_3$, 293 K, Fig. S50†): δ −3.96 (s). ESI-MS(+) (major positive ions, CH_3CN), *m*/*z* (%): 587 (100) $[(L^{Ph})Cu(PPh_3) + K]^+$. ESI-MS (−) (major negative ions, CH_3CN), *m*/*z* (%): 223 (100) $[L^{Ph}]^-$. Elemental analysis calculated for $C_{51}H_{41}CuO_2P_2$: C 75.50, H 5.09; found: C 74.11, H 4.62.

*[Ag(L^{Ph})(PPh$_3$)$_2$] (**10**).* Triphenylphosphine (2.000 mmol, 0.524 g) was solubilized in methanol (50 mL) and $AgNO_3$ (1.000 mmol, 0.170 g) was added. The reaction mixture was stirred in the dark for 2 hours. Successively, the ligand NaL^{Ph} (1.000 mmol, 0.246 g) and the mixture was left under constant magnetic stirring in the dark for 4 hours. The solution was then filtered, and the precipitate was dried under reduced pressure to give the yellow-orange complex **10** in 54% yield. A batch of good quality crystals of $[Ag(L^{Ph})(PPh_3)_2]$, suitable for X-ray analysis, was obtained by slow evaporation of a chloroform/hexane solution of **10**. M.p.: 193–197 °C. FT-IR (cm^{-1}, Fig. S51†): 3071mbr, 3045mbr, 3004br (CH); 1598m, 1557m (C=O); 1505s, 1477m, 1453s, 1434s, 1407sbr, 1333m, 1300m, 1258m, 1216m, 1178m, 1160m, 1093m, 1066m, 1026m, 1019m, 966m, 933m, 933m, 921m, 912m, 841m, 780m, 737s, 720s, 705s. ^{1}H-NMR ($CDCl_3$, 293 K, Fig. S52†): δ 6.41 (s, 1H, COC*H*CO), 7.29–7.40 (m, 23H, C*H*$_{ar}$), 7.46–7.50 (m, 13H, C*H*$_{ar}$), 7.85 (t, 4H, C*H*$_{ar}$). ^{1}H-NMR (DMSO-d_6, 293 K, Fig. S53†): δ 6.41 (s, 1H, COC*H*CO), 7.34–7.38 (m, 23H, C*H*$_{ar}$), 7.39–7.47 (m, 13H, C*H*$_{ar}$), 7.84 (t, 4H, C*H*$_{ar}$). $^{13}C\{^1H\}$-NMR ($CDCl_3$, 293 K, Fig. S54†): δ 93.38 (CO*C*HCO); 127.02, 127.18, 127.78, 128.45, 128.55, 128.69, 128.71, 132.08, 132.16, 133.93, 134.05, 134.14 (*C*H_{ar} and C_{ar}); 186.02 (*C*O). $^{31}P\{^1H\}$-NMR ($CDCl_3$, 293 K, Fig. S55†): δ 7.24 (s). $^{31}P\{^1H\}$-NMR ($CDCl_3$, 223 K, Fig. S56†): δ 7.21 (dbr, $^1J(Ag–^{31}P)$ = 439 Hz). ESI-MS(+) (major positive ions, CH_3CN), *m*/*z* (%): 633 (100) $[Ag(PPh_3)_2]^+$. Elemental analysis calculated for $C_{51}H_{41}AgO_2P_2$: C 71.59, H 4.89; found: C 71.14, H 4.58.

*[Ag(L^{Ph})(PTA)]·H$_2$O (**11**).* 1,3,4-Triazaphosphaadamantane (2.000 mmol, 0.314 g) was solubilized in methanol (30 mL) and $AgNO_3$ (1.000 mmol, 0.170 g) was added. The reaction mixture was stirred in the dark at room temperature for 2 hours. Successively, the ligand NaL^{Ph} (1.000 mmol, 0.246 g) was added and the solution was stirred in the dark at room temperature for 4 hours. The mixture was then filtered and the precipitate was dried under reduced pressure. The orange product was recovered to give complex **11** in 81% yield. M.p.: 198–203 °C. FT-IR (cm^{-1}, Fig. S57†): 3225mbr (O–H); 3060mbr, 2942mbr (C–H); 1598s, 1555s (C=O); 1513s, 1466s, 1419vs, 1345vsbr, 1289vs, 1242s, 1225s, 1180mbr, 1102s, 1069m, 1039m, 1013s, 971vs, 947vs, 898s, 843m, 828m, 804m, 790m, 745vs, 712vs. ^{1}H-NMR (CD_3OD, 293 K, Fig. S58†): δ 4.25 (d, 6H, PC*H*$_2$N), 4.56–4.67 (m, 6H, NC*H*$_2$N), 4.86 (*H*$_2$O), 6.78 (br, 1H, COC*H*CO), 7.48 (s, 5H, C*H*$_{ar}$), 7.95 (s, 5H, C*H*$_{ar}$). ^{1}H-NMR (D_2O, 293 K, Fig. S59†): δ 4.08 (d, 6H, PC*H*$_2$N), 4.45–4.51 (m, 6H, NC*H*$_2$N), 6.32 (s, 1H, COC*H*CO), 7.42–7.43 (s, 5H, C*H*$_{ar}$), 7.73 (s, 5H, C*H*$_{ar}$). ^{1}H-NMR (DMSO, 293 K, Fig. S60†): δ 4.13 (d, 6H, PC*H*$_2$N), 4.39–4.55 (m, 6H, NC*H*$_2$N), 6.45 (s, 1H, COC*H*CO), 7.42 (s, 5H, C*H*$_{ar}$), 7.90 (s, 5H, C*H*$_{ar}$). $^{13}C\{^1H\}$-NMR (CD_3OD, 293 K, Fig. S61†): 50.10 (P*C*H$_2$N); 72.00, 72.05 (NC*H*$_2$N); 90.35 (COC*H*CO); 126.76, 127.28, 128.07, 128.29, 128.36, 128.84 (*C*H_{ar} and C_{ar}), 179.93 (*C*O). $^{31}P\{^1H\}$-NMR (CD_3OD, 293 K, Fig. S62†): δ −83.82 (s). $^{31}P\{^1H\}$-NMR (CD_3OD, 223 K, Fig. S63†): δ −81.5 (br). ESI-MS(+) (major positive ions, CH_3OH), *m*/*z* (%): 158 (100) $[PTA + H]^+$, 421 (8) $[Ag(PTA)_2]^+$. Elemental analysis (%) calculated for $C_{21}H_{25}AgN_3O_3P$: N 8.30, C 49.82, H 4.98; found: N 8.95, C 48.93, H 4.88.

X-ray structure determination

A suitable crystal covered with a layer of hydrocarbon/Paratone-N oil was selected and mounted on a Cryo-loop, and immediately placed in a low temperature nitrogen stream. The X-ray intensity data of HL^{CF3} and $[Cu(L^{CF3})(PPh_3)_2]$ were measured at 100 K on a SMART APEX II CCD area detector system while X-ray intensity data of $[Ag(L^{Ph})(PPh_3)_2]$ were measured at 100(2) K on a Bruker D8 Quest equipped with a PHOTON II 7 CPAD detector. These systems were equipped with an Oxford Cryosystems 700 series cooler, a graphite monochromator, and a Mo Kα fine-focus sealed tube (λ = 0.71073 Å). Intensity data were processed using the Bruker Apex program suite. Absorption corrections were applied by using SADABS.[116] Initial atomic positions were located using SHELXT,[117] and the structures of the compounds were refined by the least-squares method using SHELXL[118] within Olex2 GUI.[119] All the non-hydrogen atoms were refined anisotropically. Hydrogen atoms were included at calculated positions and refined using appropriate riding models. The molecule HL^{CF3} sites on a two-fold rotation axis and the O–H position

are therefore disordered over two oxygen sites. $[Cu(L^{CF3})(PPh_3)_2]$ crystallizes in the $P\bar{1}$ space group with two chemically similar molecules in the asymmetric unit. X-ray structural figures were generated using Olex2. CCDC 2279297–2279299 files contain the supplementary crystallography data. Additional details are provided in the ESI.† We have also recorded single crystal X-ray data of $[Cu(L^{Mes})(PPh_3)_2]$ and obtained its molecular structure. Unfortunately, the crystal quality is poor and also suffers due to twinning. As a result, the structure is not of sufficient quality for a detailed analysis of metrical parameters. The atom connectivity and basic features of the molecule are however clear from the data (see the ESI, Tables S1–S9†).

Experiments with cultured human cancer cells

Ag(I) and Cu(I) complexes and the corresponding uncoordinated ligands and related salts were dissolved in DMSO just before the experiment, and a calculated volume of the drug solution was added to the cell growth medium to a final solvent concentration of 0.5%, which had no detectable effects on cell viability. Cisplatin was dissolved in 0.9% sodium chloride solution. MTT (3-(4,5-dimethylthiazol-2-yl)-2,5-diphenyltetrazolium bromide) and cisplatin were obtained from Sigma Chemical Co, St Louis, MO, USA.

Cell cultures

Human SCLC (U1285), NSCLC (A549), testicular (NTERA-2), colon (HCT-15), and pancreatic (PSN-1 and BxPC3) carcinoma cell lines were obtained from American Type Culture Collection (ATCC, Rockville, MD, USA). Cell lines were maintained in the logarithmic phase at 37 °C under a 5% carbon dioxide atmosphere using the RPMI-1640 medium (EuroClone, Milan, Italy) containing 10% fetal calf serum (EuroClone, Milan, Italy), antibiotics (50 units per mL penicillin and 50 μg mL^{-1} streptomycin) and 2 mM L-glutamine.

MTT assay

The growth inhibitory effect toward tumor cells was evaluated by means of the MTT assay as previously described.[85] IC_{50} values, the drug concentrations that reduce the mean absorbance at 570 nm to 50% of those in the untreated control wells, were calculated using the four-parameter logistic (4-PL) model. The evaluation was based on means from at least three independent experiments.

Spheroid cultures and acid phosphatase (APH) assay

Spheroid cultures were obtained by seeding 2.5×10^3 HCT-15 human cancer cells per well in a round-bottom non-treated tissue culture 96-well plate (Greiner Bio-one, Kremsmünster, Austria) in a phenol red free RPMI-1640 medium (Sigma Chemical Co., St Louis, MO, USA) containing 10% fetal calf serum supplemented with 20% methyl cellulose stock solution. An APH modified assay was employed for evaluating cell viability in 3D spheroids, as previously described.[85] IC_{50} values (drug concentrations that reduce the mean absorbance at 405 nm to 50% of those in the untreated control wells) were calculated using the 4-PL model. The evaluation was based on means from at least three independent experiments.

Conflicts of interest

The authors declare no competing financial interests.

Acknowledgements

This work was supported by Unione Europea - NextGenerationEU (MUR-Fondo Promozione e Sviluppo - D.M. 737/2021, INVIRCuM, University of Camerino, FAR 2022 PNR, and NGEU PNRR, D.M. n. 351/2022 M4C1 I4.1) and by the University of Padova (PRID BIRD225980). H.V.R.D. acknowledges the support by the National Science Foundation through grant CHE-1954456.

References

1 K. D. Mjos and C. Orvig, *Chem. Rev.*, 2014, **114**, 4540–4563.
2 N. P. E. Barry and P. J. Sadler, *Chem. Commun.*, 2013, **49**, 5106–5131.
3 *Metal-based Anticancer Agents*, ed. A. Casini, A. Vessières and S. M. Meier-Menches, The Royal Society of Chemistry, Croydon, UK, 2019.
4 *Metallo-Drugs: Development and Action of Anticancer Agents*, ed. A. Sigel, E. Freisinger and R. K. O. Sigel, De Gruyter, 2018.
5 S. Medici, M. Peana, V. M. Nurchi and M. A. Zoroddu, *J. Med. Chem.*, 2019, **62**, 5923–5943.
6 C. Santini, M. Pellei, V. Gandin, M. Porchia, F. Tisato and C. Marzano, *Chem. Rev.*, 2014, **114**, 815–862.
7 S. Nobili, E. Mini, I. Landini, C. Gabbiani, A. Casini and L. Messori, *Med. Res. Rev.*, 2010, **30**, 550–580.
8 J. A. Joule and K. Mills, *Heterocyclic Chemistry*, Wiley, Chichester (UK), Fifth edn, 2010.
9 C. Y. Chen, J. C. Lien, C. Y. Chen, C. C. Hung and H. C. Lin, *Int. J. Mol. Sci.*, 2021, **22**, 12171.
10 C. Pettinari, F. Marchetti and A. Drozdov, in *Compr. Coord. Chem. II*, ed. J. A. McCleverty and T. J. Meyer, Pergamon, Oxford, 2003, pp. 97–115.
11 A. R. Siedle, in *Compr. Coord. Chem*, ed. G. Wilkinson, R. D. Gillard and J. A. McCleverty, Pergamon, Oxford, UK, 1987, pp. 365–412.
12 A. S. Crossman and M. P. Marshak, in *Compr. Coord. Chem. III*, ed. E. C. Constable, G. Parkin and L. Que Jr, Elsevier, Oxford, 2021, pp. 331–365.
13 M. Stalpaert and D. De Vos, *ACS Sustainable Chem. Eng.*, 2018, **6**, 12197–12204.
14 A. S. Crossman, A. T. Larson, J. X. Shi, S. M. Krajewski, E. S. Akturk and M. P. Marshak, *J. Org. Chem.*, 2019, **84**, 7434–7442.

15 S. M. Krajewski, A. S. Crossman, E. S. Akturk, T. Suhrbier, S. J. Scappaticci, M. W. Staab and M. P. Marshak, *Dalton Trans.*, 2019, **48**, 10714–10722.
16 E. S. Akturk, S. J. Scappaticci, R. N. Seals and M. P. Marshak, *Inorg. Chem.*, 2017, **56**, 11466–11469.
17 T. Schilling, K. B. Keppler, M. E. Heim, G. Niebch, H. Dietzfelbinger, J. Rastetter and A. R. Hanauske, *Invest. New Drugs*, 1995, **13**, 327–332.
18 H. Bischoff, M. R. Berger, B. K. Keppler and D. Schmähl, *J. Cancer Res. Clin. Oncol.*, 1987, **113**, 446–450.
19 A. Wu, D. C. Kennedy, B. O. Patrick and B. R. James, *Inorg. Chem. Commun.*, 2003, **6**, 996–1000.
20 R. Fernández, M. Melchart, A. Habtemariam, S. Parsons and P. J. Sadler, *Chem. – Eur. J.*, 2004, **10**, 5173–5179.
21 M. Melchart, A. Habtemariam, S. Parsons and P. J. Sadler, *J. Inorg. Biochem.*, 2007, **101**, 1903–1912.
22 C. A. Vock, A. K. Renfrew, R. Scopelliti, L. Juillerat-Jeanneret and P. J. Dyson, *Eur. J. Inorg. Chem.*, 2008, 1661–1671.
23 C. Aliende, M. Pérez-Manrique, F. A. Jalón, B. R. Manzano, A. M. Rodríguez, J. V. Cuevas, G. Espino, M. Á. Martínez, A. Massaguer, M. González-Bártulos, R. De Llorens and V. Moreno, *J. Inorg. Biochem.*, 2012, **117**, 171–188.
24 S. Seršen, J. Kljun, K. Kryeziu, R. Panchuk, B. Alte, W. Körner, P. Heffeter, W. Berger and I. Turel, *J. Med. Chem.*, 2015, **58**, 3984–3996.
25 J. Kljun and I. Turel, *Eur. J. Inorg. Chem.*, 2017, **2017**, 1655–1666.
26 J. Conradie and J. C. Swarts, *Dalton Trans.*, 2011, **40**, 5844–5851.
27 J. Conradie and J. C. Swarts, *Eur. J. Inorg. Chem.*, 2011, **2011**, 2439–2449.
28 J. Do Couto Almeida, I. M. Marzano, F. C. S. De Paula, M. Pivatto, N. P. Lopes, P. C. De Souza, F. R. Pavan, A. L. B. Formiga, E. C. Pereira-Maia and W. Guerra, *J. Mol. Struct.*, 2014, **1075**, 370–376.
29 D. I. Ugwu and J. Conradie, *J. Inorg. Biochem.*, 2023, 112268.
30 A. Muscella, N. Calabriso, C. Vetrugno, F. P. Fanizzi, S. A. De Pascali, C. Storelli and S. Marsigliante, *Biochem. Pharmacol.*, 2011, **81**, 91–103.
31 A. Muscella, N. Calabriso, C. Vetrugno, F. P. Fanizzi, S. A. De Pascali and S. Marsigliante, *Biochem. Pharmacol.*, 2011, **81**, 1271–1285.
32 A. Muscella, N. Calabriso, C. Vetrugno, L. Urso, F. P. Fanizzi, S. A. De Pascali and S. Marsigliante, *Br. J. Pharmacol.*, 2010, **160**, 1362–1377.
33 A. Muscella, N. Calabriso, F. P. Fanizzi, S. A. De Pascali, L. Urso, A. Ciccarese, D. Migoni and S. Marsigliante, *Br. J. Pharmacol.*, 2008, **153**, 34–49.
34 K. Nakano, T. Nakayachi, E. Yasumoto, S. R. Morshed, K. Hashimoto, H. Kikuchi, H. Nishikawa, K. Sugiyama, O. Amano, M. Kawase and H. Sakagami, *Anticancer Res.*, 2004, **24**, 711–717.
35 J. J. Wilson and S. J. Lippard, *J. Med. Chem.*, 2012, **55**, 5326–5336.
36 S. A. Gromilov and I. A. Baidina, *J. Struct. Chem.*, 2004, **45**, 1031–1081.
37 L. G. Bulusheva, A. V. Okotrub, T. I. Liskovskaya, S. A. Krupoder, A. V. Guselnikov, A. V. Manaev and V. F. Traven, *J. Phys. Chem. A*, 2001, **105**, 8200–8205.
38 K. M. Chi, H. K. Shin, M. J. Hampden-Smith, E. N. Duesler and T. T. Kodas, *Polyhedron*, 1991, **10**, 2293–2299.
39 A. T. Larson, A. S. Crossman, S. M. Krajewski and M. P. Marshak, *Inorg. Chem.*, 2020, **59**, 423–432.
40 H. Lang, M. Leschke, M. Melter, B. Walfort, K. Kohler, S. E. Schulz and T. Gessner, *Z. Anorg. Allg. Chem.*, 2003, **629**, 2371–2380.
41 H. K. Shin, K. M. Chi, J. Farkas, M. J. Hampden-Smith, T. T. Kodas and E. N. Duesler, *Inorg. Chem.*, 1992, **31**, 424–431.
42 K.-M. Chi, J. Farkas, M. J. Hampden-Smith, T. T. Kodas and E. N. Duesler, *Dalton Trans.*, 1992, 3111–3117.
43 H. K. Shin, M. J. Hampden-Smith, E. N. Duesler and T. T. Kodas, *Can. J. Chem.*, 1992, **70**, 2954–2966.
44 T. H. Baum and C. E. Larson, *Chem. Mater.*, 1992, **4**, 365–369.
45 S. K. Reynolds, C. J. Smart, E. F. Baran, T. H. Baum, C. E. Larson and P. Brock, *Appl. Phys. Lett.*, 1991, **59**, 2332.
46 D. B. Beach, F. K. LeGoues and C. K. Hu, *Chem. Mater.*, 1990, **2**, 216–219.
47 Y. L. Chow and G. E. Buono-Core, *Can. J. Chem.*, 1983, **61**, 795–800.
48 R. J. Restivo, A. Costin, G. Ferguson and A. J. Carty, *Can. J. Chem.*, 1975, **53**, 1949–1957.
49 W. A. Anderson, A. J. Carty, G. J. Palenik and G. Schreiber, *Can. J. Chem.*, 1971, **49**, 761–766.
50 A. Jakob, C. C. Joubert, T. Rüffer, J. C. Swarts and H. Lang, *Inorg. Chim. Acta*, 2014, **411**, 48–55.
51 P. Tasker, A. Parkin, T. C. Higgs, S. Parsons and D. Messanger, *CSD communication (private communication)*, 2005.
52 R.-N. Yang, D.-M. Wang, Y.-F. Liu and D.-M. Jin, *Polyhedron*, 2001, **20**, 585–590.
53 S. A. Gulyaev, E. S. Vikulova, T. S. Sukhikh, I. Y. Ilyin and N. B. Morozova, *J. Struct. Chem.*, 2021, **62**, 1836–1845.
54 I. S. Fedoseev, E. S. Vikulova, I. Y. Il'in, A. I. Smolentsev, M. R. Gallyamov and N. B. Morozova, *J. Struct. Chem.*, 2016, **57**, 1667–1670.
55 K. Akhbari and A. Morsali, *Cryst. Growth Des.*, 2007, **7**, 2024–2030.
56 W. J. Evans, D. G. Giarikos, D. Josell and J. W. Ziller, *Inorg. Chem.*, 2003, **42**, 8255–8261.
57 C. Y. Xu, T. S. Corbitt, M. J. Hampdensmith, T. T. Kodas and E. N. Duesler, *Dalton Trans.*, 1994, 2841–2849.
58 E. S. Vikulova, T. S. Sukhikh, S. A. Gulyaev, I. Y. Ilyin and N. B. Morozova, *Molecules*, 2022, **27**, 677.
59 F. Marandi, M. Ghadermazi, A. Marandi, I. Pantenburg and G. Meyer, *J. Mol. Struct.*, 2011, **1006**, 136–141.
60 A. J. Blake, N. R. Champness, S. M. Howdle, K. S. Morley, P. B. Webb and C. Wilson, *CrystEngComm*, 2002, **4**, 88–92.

61 Y. L. Shen, J. L. Jin, G. X. Duan, P. Y. Yu, Y. P. Xie and X. Lu, *Chem. – Eur. J.*, 2021, **27**, 1122–1126.
62 J. L. Jin, Y. P. Xie, H. Cui, G. X. Duan, X. Lu and T. C. W. Mak, *Inorg. Chem.*, 2017, **56**, 10412–10417.
63 H. Liu, S. Battiato, A. L. Pellegrino, P. Paoli, P. Rossi, C. Jimenez, G. Malandrino and D. Munoz-Rojas, *Dalton Trans.*, 2017, **46**, 10986–10995.
64 A. O. Rybaltovskii, V. G. Arakcheev, A. N. Bekin, A. F. Danilyuk, V. I. Gerasimova, N. V. Minaev, E. N. Golubeva, O. O. Parenago and V. N. Bagratashvili, *Russ. J. Phys. Chem. B*, 2015, **9**, 1137–1142.
65 G. Calabrese, S. Petralia, D. Franco, G. Nocito, C. Fabbi, L. Forte, S. Guglielmino, S. Squarzoni, F. Traina and S. Conoci, *Mater. Sci. Eng., C*, 2021, **118**, 111394.
66 H. Schmidt, A. Jakob, T. Haase, K. Kohse-Hoinghaus, S. E. Schulz, T. Wachtler, T. Gessner and H. Lang, *Z. Anorg. Allg. Chem.*, 2005, **631**, 2786–2791.
67 D. A. Edwards, R. M. Harker, M. F. Mahon and K. C. Molloy, *J. Mater. Chem.*, 1999, **9**, 1771–1780.
68 Z. Yuan, N. H. Dryden, J. J. Vittal and R. J. Puddephatt, *Chem. Mater.*, 1995, **7**, 1696–1702.
69 Z. Yuan, N. H. Dryden, J. J. Vittal and R. J. Puddephatt, *Can. J. Chem.*, 1994, **72**, 1605–1609.
70 N. H. Dryden, J. J. Vittal and R. J. Puddephatt, *Chem. Mater.*, 1993, **5**, 765–766.
71 W. Lin, T. H. Warren, R. G. Nuzzo and G. S. Girolami, *J. Am. Chem. Soc.*, 1993, **115**, 11644–11645.
72 S. Wanninger, V. Lorenz, A. Subhan and F. T. Edelmann, *Chem. Soc. Rev.*, 2015, **44**, 4986–5002.
73 M. H. M. Leung, T. Harada and T. W. Kee, *Curr. Pharm. Des.*, 2013, **19**, 2070–2083.
74 Y. Figueroa-DePaz, K. Resendiz-Acevedo, S. G. Dávila-Manzanilla, J. C. García-Ramos, L. Ortiz-Frade, J. Serment-Guerrero and L. Ruiz-Azuara, *J. Inorg. Biochem.*, 2022, **231**, 111772.
75 J. Serment-Guerrero, M. E. Bravo-Gomez, E. Lara-Rivera and L. Ruiz-Azuara, *J. Inorg. Biochem.*, 2017, **166**, 68–75.
76 I. Correia, S. Borovic, I. Cavaco, C. P. Matos, S. Roy, H. M. Santos, L. Fernandes, J. L. Capelo, L. Ruiz-Azuara and J. C. Pessoa, *J. Inorg. Biochem.*, 2017, **175**, 284–297.
77 L. Ruiz-Azuara and M. E. Bravo-Gomez, *Curr. Med. Chem.*, 2010, **17**, 3606–3615.
78 L. Polloni, A. C. D. Silva, S. C. Teixeira, F. V. D. Azevedo, M. A. P. Zoia, M. S. da Silva, P. Lima, L. I. V. Correia, J. D. Almeida, C. V. da Silva, V. D. R. Avila, L. R. F. Goulart, S. Morelli, W. Guerra and R. J. de Oliveira, *Biomed. Pharmacother.*, 2019, **112**, 108586.
79 D. A. Paixao, B. C. A. de Oliveira, J. D. Almeida, L. M. Sousa, C. D. Lopes, Z. A. Carneiro, D. Y. Tezuka, J. C. T. Clavijo, J. Ellena, L. Polloni, P. H. A. Machado, S. de Albuquerque, R. J. de Oliveira, S. Guilardi and W. Guerra, *Inorg. Chim. Acta*, 2020, **499**, 119164.
80 R. E. Malekshah, M. Salehi, M. Kubicki and A. Khaleghian, *J. Coord. Chem.*, 2019, **72**, 1697–1714.
81 R. E. Malekshah, M. Salehi, M. Kubicki and A. Khaleghian, *J. Coord. Chem.*, 2018, **71**, 952–968.
82 A. Pramanik, D. Laha, P. Pramanik and P. Karmakar, *J. Drug Targeting*, 2014, **22**, 23–33.
83 D. F. Xu, Z. H. Shen, Y. Shi, Q. He and Q. C. Xia, *Russ. J. Coord. Chem.*, 2010, **36**, 458–462.
84 L. A. Khamidullina, I. S. Puzyrev, G. L. Burygin, P. V. Dorovatovskii, Y. V. Zubavichus, A. V. Mitrofanova, V. N. Khrustalev, T. V. Timofeeva, P. A. Slepukhin, P. D. Tobysheva, A. V. Pestov, E. Solari, A. G. Tskhovrebov and V. G. Nenajdenko, *Molecules*, 2021, **26**, 6466.
85 M. Pellei, C. Santini, L. Bagnarelli, M. Caviglia, P. Sgarbossa, M. De Franco, M. Zancato, C. Marzano and V. Gandin, *Int. J. Mol. Sci.*, 2023, **24**, 4091.
86 F. Del Bello, M. Pellei, L. Bagnarelli, C. Santini, G. Giorgioni, A. Piergentili, W. Quaglia, C. Battocchio, G. Iucci, I. Schiesaro, C. Meneghini, I. Venditti, N. Ramanan, M. De Franco, P. Sgarbossa, C. Marzano and V. Gandin, *Inorg. Chem.*, 2022, **61**, 4919–4937.
87 M. Pellei, L. Bagnarelli, L. Luciani, F. Del Bello, G. Giorgioni, A. Piergentili, W. Quaglia, M. De Franco, V. Gandin, C. Marzano and C. Santini, *Int. J. Mol. Sci.*, 2020, **21**, 2616.
88 M. B. Morelli, C. Amantini, G. Santoni, M. Pellei, C. Santini, C. Cimarelli, E. Marcantoni, M. Petrini, F. Del Bello, G. Giorgioni, A. Piergentili and W. Quaglia, *New J. Chem.*, 2018, **42**, 11878–11887.
89 V. Gandin, C. Ceresa, G. Esposito, S. Indraccolo, M. Porchia, F. Tisato, C. Santini, M. Pellei and C. Marzano, *Sci. Rep.*, 2017, **7**, 13936.
90 F. Tisato, C. Marzano, V. Peruzzo, M. Tegoni, M. Giorgetti, M. Damjanovic, A. Trapananti, A. Bagno, C. Santini, M. Pellei, M. Porchia and V. Gandin, *J. Inorg. Biochem.*, 2016, **165**, 80–91.
91 G. Papini, G. Bandoli, A. Dolmella, G. Gioia Lobbia, M. Pellei and C. Santini, *Inorg. Chem. Commun.*, 2008, **11**, 1103–1106.
92 M. Inoue, Y. Sumii and N. Shibata, *ACS Omega*, 2020, **5**, 10633–10640.
93 E. P. Gillis, K. J. Eastman, M. D. Hill, D. J. Donnelly and N. A. Meanwell, *J. Med. Chem.*, 2015, **58**, 8315–8359.
94 S. Purser, P. R. Moore, S. Swallow and V. Gouverneur, *Chem. Soc. Rev.*, 2008, **37**, 320–330.
95 P. Shah and A. D. Westwell, *J. Enzyme Inhib. Med. Chem.*, 2007, **22**, 527–540.
96 L. H. Doerrer and H. V. R. Dias, *Dalton Trans.*, 2023, **52**, 7770–7771.
97 S. Swallow, in *Prog. Med. Chem*, ed. G. Lawton and D. R. Witty, Elsevier, 2015, vol. 54, pp. 65–133.
98 I. M. Abdou, A. M. Saleh and H. F. Zohdi, *Molecules*, 2004, **9**, 109–116.
99 P. N. Edwards, in *Organofluorine Chemistry: Principles and Commercial Applications*, ed. R. E. Banks, B. E. Smart and J. C. Tatlow, Springer US, Boston, MA, 1994, pp. 501–541.
100 C. R. Groom, I. J. Bruno, M. P. Lightfoot and S. C. Ward, *Acta Crystallogr., Sect. B: Struct. Sci., Cryst. Eng. Mater.*, 2016, **72**, 171–179.

101 J. S. Lakhi, M. R. Patterson and H. V. R. Dias, *New J. Chem.*, 2020, **44**, 14814–14822.
102 C. Zhang, P. Yang, Y. Yang, X. Huang, X.-J. Yang and B. Wu, *Synth. Commun.*, 2008, **38**, 2349–2356.
103 J. Emsley, in *Complex Chemistry. Structure and Bonding*, ed. J. Emsley, R. D. Ernst, B. J. Hathaway and K. D. Warren, Springer, Berlin, Heidelberg, 1984, vol. 57, pp. 147–191.
104 M. A. Halcrow, J.-S. Sun, J. C. Huffman and G. Christou, *Inorg. Chem.*, 1995, **34**, 4167–4177.
105 R. P. Dryden and A. Winston, *J. Phys. Chem.*, 1958, **62**, 635–637.
106 B. Cheng, H. Yi, C. He, C. Liu and A. Lei, *Organometallics*, 2014, **34**, 206–211.
107 C. He, G. Zhang, J. Ke, H. Zhang, J. T. Miller, A. J. Kropf and A. Lei, *J. Am. Chem. Soc.*, 2013, **135**, 488–493.
108 S. N. Slabzhennikov, O. B. Ryabchenko and L. A. Kuarton, *Russ. J. Coord. Chem.*, 2006, **32**, 545–551.
109 A. Guerriero, M. Peruzzini and L. Gonsalvi, *Coord. Chem. Rev.*, 2018, **355**, 328–361.
110 A. M. Kirillov, S. W. Wieczorek, M. F. C. Guedes da Silva, J. Sokolnicki, P. Smoleński and A. J. L. Pombeiro, *CrystEngComm*, 2011, **13**, 6329–6333.
111 H. V. R. Dias, J. A. Flores, M. Pellei, B. Morresi, G. Gioia Lobbia, S. Singh, Y. Kobayashi, M. Yousufuddin and C. Santini, *Dalton Trans.*, 2011, **40**, 8569–8580.
112 M. Pellei, S. Alidori, G. Papini, G. Gioia Lobbia, J. D. Gorden, H. V. R. Dias and C. Santini, *Dalton Trans.*, 2007, 4845–4853.
113 H. V. R. Dias, S. Alidori, G. Gioia Lobbia, G. Papini, M. Pellei and C. Santini, *Inorg. Chem.*, 2007, **46**, 9708–9714.
114 V. Gandin, F. Tisato, A. Dolmella, M. Pellei, C. Santini, M. Giorgetti, C. Marzano and M. Porchia, *J. Med. Chem.*, 2014, **57**, 4745–4760.
115 S. El Harane, B. Zidi, N. El Harane, K.-H. Krause, T. Matthes and O. Preynat-Seauve, *Journal*, 2023, **12**, 1001.
116 L. Krause, R. Herbst-Irmer, G. M. Sheldrick and D. Stalke, *J. Appl. Crystallogr.*, 2015, **48**, 3–10.
117 G. M. Sheldrick, *Acta Crystallogr., Sect. A: Found. Adv.*, 2015, **71**, 3–8.
118 G. M. Sheldrick, *Acta Crystallogr., Sect. C: Struct. Chem.*, 2015, **71**, 3–8.
119 O. V. Dolomanov, L. J. Bourhis, R. J. Gildea, J. A. K. Howard and H. Puschmann, *J. Appl. Crystallogr.*, 2009, **42**, 339–341.